### Reporter plasmids, transient transfection, and dual luciferase assays

The firefly luciferase reporter plasmid was used to examine let7g and miRNA93 function. pGL4-TK, a renilla luciferase reporter, was used as an internal control [44]. Transfection and dual luciferase assays were performed as described previously [45].

### Flow cytometry

The expression levels of MICA on the cell surface were determined using flow cytometry, as described previously [23]. Briefly, cells were hybridized with anti-MICA (1:500; R&D Systems, Minneapolis, MN, USA) and isotype control IgG (1:500; R&D Systems) in 5% BSA/1% sodium azide/PBS for 1 h at 4°C. After washing, cells were incubated with goat anti-mouse Alexa 488 (1:1,000; Molecular Probes, Eugene, OR, USA) for 30 min. Flow cytometry was performed and the data analyzed using Guava Easy Cyte Plus (GE Healthcare, Little Chalfont, UK).

### ELISA for MICA

The concentration of MICA in the cell culture supernatant was measured using a sandwich ELISA, according to the manufacturer's instructions (R&D Systems, Minneapolis, MN, USA).

### Statistical analysis

Significant differences between groups were determined using the Student's *t*-test when variances were equal and using Welch's *t*-test when variances were unequal. *P*-values less than 0.05 were considered statistically significant.

## ACKNOWLEDGMENTS

This work was supported by Grants-in-Aid from the Ministry of Education, Culture, Sports, Science and Technology, Japan (# 25293076 and #24390183) (to M.Otsuka and K.K.); Health Sciences Research Grants from the Ministry of Health, Labour and Welfare of Japan (Research on Hepatitis) (to S.K. and K.K.); the Program for Promotion of Basic and Applied Researches for Innovations in Bio-oriented Industry (BRAIN) (to S.K.); grants from the Okinaka Memorial Institute for Medical Research, the Liver Forum in Kyoto, and the Japanese Society of Gastroenterology (to M.Otsuka).

### Editorial note

This paper has been accepted based in part on peer-review conducted by another journal and the authors' response and revisions as well as expedited peer-review in Oncotarget

## AUTHOR CONTRIBUTIONS

M.Ohno and M.Otsuka planned the research and wrote the manuscript. M.Ohno, T.K., C.S., T.Y., and A.T. performed the majority of the experiments. R.M., N.K., M.S. and N.K. measured performed ELISA. S.K. provided materials and wrote the manuscript. K.K. supervised the entire project.

## COMPETING FINANCIAL INTERESTS

The authors declare no competing financial interests.

## REFERENCES

1 Mittal S, El-Serag HB: Epidemiology of hepatocellular carcinoma: Consider the population. J Clin Gastroenterol 2013;47 Suppl:S2-6.

2 Chen DS: From hepatitis to hepatoma: Lessons from type b viral hepatitis. Science 1993;262:369-370.

3 Blachier M, Leleu H, Peck-Radosavljevic M, Valla DC, Roudot-Thoraval F: The burden of liver disease in europe: A review of available epidemiological data. J Hepatol 2013;58:593-608.

4 Yuen MF, Lai CL: Treatment of chronic hepatitis b: Evolution over two decades. J Gastroenterol Hepatol 2011;26 Suppl 1:138-143.

5 Liaw YF, Chu CM: Hepatitis b virus infection. Lancet 2009;373:582-592.

6 Omata M: Treatment of chronic hepatitis b infection. N Engl J Med 1998;339:114-115.

7 Tuttleman JS, Pourcel C, Summers J: Formation of the pool of covalently closed circular viral dna in hepadnavirus-infected cells. Cell 1986;47:451-460.

8 Sureau C, Romet-Lemonne JL, Mullins JI, Essex M: Production of hepatitis b virus by a differentiated human hepatoma cell line after transfection with cloned circular hbv dna. Cell 1986;47:37-47.

9 Günther S, Li BC, Miska S, Krüger DH, Meisel H, Will H: A novel method for efficient amplification of whole hepatitis b virus genomes permits rapid functional analysis and reveals deletion mutants in immunosuppressed patients. J Virol 1995;69:5437-5444.

10 Summers J, Mason WS: Replication of the genome of a hepatitis b--like virus by reverse transcription of an rna intermediate. Cell 1982;29:403-415.

11 Chang CM, Jeng KS, Hu CP, Lo SJ, Su TS, Ting LP, Chou CK, Han SH, Pfaff E, Salfeld J: Production of hepatitis b virus in vitro by transient expression of cloned hbv dna in a hepatoma cell line. EMBO J 1987;6:675-680.

12 Delaney WE, Isom HC: Hepatitis b virus replication in human hepg2 cells mediated by hepatitis b virus recombinant baculovirus. Hepatology 1998;28:1134-1146.

13 Mercer DF, Schiller DE, Elliott JF, Douglas DN, Hao C, Rinfret A, Addison WR, Fischer KP, Churchill TA, Lakey JR, Tyrrell DL, Kneteman NM: Hepatitis c virus replication in mice with chimeric human livers. Nat Med 2001;7:927-933.

14 Chayama K, Hayes CN, Hiraga N, Abe H, Tsuge M, Imamura M: Animal model for study of human hepatitis viruses. J Gastroenterol Hepatol 2011;26:13-18.

15 Meuleman P, Libbrecht L, De Vos R, de Hemptinne B, Gevaert K, Vandekerckhove J, Roskams T, Leroux-Roels G: Morphological and biochemical characterization of a human liver in a upa-scid mouse chimera. Hepatology 2005;41:847-856.

16 Sainz B, Barretto N, Martin DN, Hiraga N, Imamura M, Hussain S, Marsh KA, Yu X, Chayama K, Alrefai WA, Uprichard SL: Identification of the niemann-pick c1-like 1 cholesterol absorption receptor as a new hepatitis c virus entry factor. Nat Med 2012;18:281-285.

17 Tsuge M, Takahashi S, Hiraga N, Fujimoto Y, Zhang Y, Mitsui F, Abe H, Kawaoka T, Imamura M, Ochi H, Hayes CN, Chayama K: Effects of hepatitis b virus infection on the interferon response in immunodeficient human hepatocyte chimeric mice. J Infect Dis 2011;204:224-228.

18 Tsuge M, Hiraga N, Takaishi H, Noguchi C, Oga H, Imamura M, Takahashi S, Iwao E, Fujimoto Y, Ochi H, Chayama K, Tateno C, Yoshizato K: Infection of human hepatocyte chimeric mouse with genetically engineered hepatitis b virus. Hepatology 2005;42:1046-1054.

19 Gripon P, Rumin S, Urban S, Le Seyec J, Glaise D, Cannie I, Guyomard C, Lucas J, Trepo C, Guguen-Guillouzo C: Infection of a human hepatoma cell line by hepatitis b virus. Proc Natl Acad Sci U S A 2002;99:15655-15660.

20 Yamada T, Jung J, Seno M, Kondo A, Ueda M, Tanizawa K, Kuroda S: Electroporation and use of hepatitis b virus envelope l proteins as bionanocapsules. Cold Spring Harb Protoc 2012;2012:702-705.

21 Yamada T, Iwasaki Y, Tada H, Iwabuki H, Chuah MK, VandenDriessche T, Fukuda H, Kondo A, Ueda M, Seno M, Tanizawa K, Kuroda S: Nanoparticles for the delivery of genes and drugs to human hepatocytes. Nat Biotechnol 2003;21:885-890.

22 Bartel DP: Micrornas: Target recognition and regulatory functions. Cell 2009;136:215-233.

23 Kishikawa T, Otsuka M, Yoshikawa T, Ohno M, Takata A, Shibata C, Kondo Y, Akanuma M, Yoshida H, Koike K: Regulation of the expression of the liver cancer susceptibility gene mica by micrornas. Sci Rep 2013;3:2739.

24 Kumar V, Kato N, Urabe Y, Takahashi A, Muroyama R, Hosono N, Otsuka M, Tateishi R, Omata M, Nakagawa H, Koike K, Kamatani N, Kubo M, Nakamura Y, Matsuda K: Genome-wide association study identifies a susceptibility locus for hcv-induced hepatocellular carcinoma. Nat Genet 2011;43:455-458.

25 Kumar V, Yi Lo PH, Sawai H, Kato N, Takahashi A, Deng Z, Urabe Y, Mbarek H, Tokunaga K, Tanaka Y, Sugiyama M, Mizokami M, Muroyama R, Tateishi R, Omata M, Koike K, Tanikawa C, Kamatani N, Kubo M, Nakamura Y, Matsuda K: Soluble mica and a mica variation as possible prognostic biomarkers for hbv-induced hepatocellular carcinoma. PLoS One 2012;7:e44743.

26 Pan XB, Ma H, Jin Q, Wei L: Characterization of microrna expression profiles associated with hepatitis b virus replication and clearance in vivo and in vitro. J Gastroenterol Hepatol 2012;27:805-812.

27 Niu Y, Wu Z, Shen Q, Song J, Luo Q, You H, Shi G, Qin W: Hepatitis b virus x protein co-activates pregnane x receptor to induce the cytochrome p450 3a4 enzyme, a potential implication in hepatocarcinogenesis. Dig Liver Dis 2013;45:1041-1048.

28 Mills JB, Rose KA, Sadagopan N, Sahi J, de Morais SM: Induction of drug metabolism enzymes and mdr1 using a novel human hepatocyte cell line. J Pharmacol Exp Ther 2004;309:303-309.

29 Stern-Ginossar N, Gur C, Biton M, Horwitz E, Elboim M, Stanietsky N, Mandelboim M, Mandelboim O: Human micrornas regulate stress-induced immune responses mediated by the receptor nkg2d. Nat Immunol 2008;9:1065-1073.

30 Yamada T, Iwabuki H, Kanno T, Tanaka H, Kawai T, Fukuda H, Kondo A, Seno M, Tanizawa K, Kuroda S: Physicochemical and immunological characterization of hepatitis b virus envelope particles exclusively consisting of the entire l (pre-s1 + pre-s2 + s) protein. Vaccine 2001;19:3154-3163.

31 Jung J, Matsuzaki T, Tatematsu K, Okajima T, Tanizawa K, Kuroda S: Bio-nanocapsule conjugated with liposomes for in vivo pinpoint delivery of various materials. J Control Release 2008;126:255-264.

32 Guo H, Ingolia NT, Weissman JS, Bartel DP: Mammalian micrornas predominantly act to decrease target mrna levels. Nature 2010;466:835-840.

33 Meister G: Mirnas get an early start on translational silencing. Cell 2007;131:25-28.

34 Chitadze G, Lettau M, Bhat J, Wesch D, Steinle A, Fürst D, Mytilineos J, Kalthoff H, Janssen O, Oberg HH, Kabelitz D: Shedding of endogenous mhc class i-related chain molecules a and b from different human tumor entities: Heterogeneous involvement of the "A disintegrin and metalloproteases" 10 and 17. Int J Cancer 2013;133:1557-1566.

35 Jung J, Iijima M, Yoshimoto N, Sasaki M, Niimi T, Tatematsu K, Jeong SY, Choi EK, Tanizawa K, Kuroda S: Efficient and rapid purification of drug- and gene-carrying bio-nanocapsules, hepatitis b virus surface antigen l particles, from saccharomyces cerevisiae. Protein Expr Purif 2011;78:149-155.

36 Honda M, Kaneko S, Kawai H, Shirota Y, Kobayashi K: Differential gene expression between chronic hepatitis b and c hepatic lesion. Gastroenterology 2001;120:955-966.

37 Otsuka M, Aizaki H, Kato N, Suzuki T, Miyamura T, Omata M, Seki N: Differential cellular gene expression induced by hepatitis b and c viruses. Biochem Biophys Res Commun 2003;300:443-447.

38 Wang X, Yuan ZH, Zheng LJ, Yu F, Xiong W, Liu JX, Hu GX, Li Y: Gene expression profiles in an hepatitis b virus transfected hepatoblastoma cell line and differentially regulated gene expression by interferon-alpha. World J Gastroenterol 2004;10:1740-1745.

39 Dandri M, Locarnini S: New insight in the pathobiology of hepatitis b virus infection. Gut 2012;61 Suppl 1:i6-17.

40 Wang H, Ryu WS: Hepatitis b virus polymerase blocks pattern recognition receptor signaling via interaction with ddx3: Implications for immune evasion. PLoS Pathog 2010;6:e1000986.

41 Fisicaro P, Valdatta C, Boni C, Massari M, Mori C, Zerbini A, Orlandini A, Sacchelli L, Missale G, Ferrari C: Early kinetics of innate and adaptive immune responses during hepatitis b virus infection. Gut 2009;58:974-982.

42 Banaudha K, Kaliszewski M, Korolnek T, Florea L, Yeung ML, Jeang KT, Kumar A: Microrna silencing of tumor suppressor dlc-1 promotes efficient hepatitis c virus replication in primary human hepatocytes. Hepatology 2011;53:53-61.

43 Yamasaki C, Tateno C, Aratani A, Ohnishi C, Katayama S, Kohashi T, Hino H, Marusawa H, Asahara T, Yoshizato K: Growth and differentiation of colony-forming human hepatocytes in vitro. J Hepatol 2006;44:749-757.

44 Takata A, Otsuka M, Yoshikawa T, Kishikawa T, Hikiba Y, Obi S, Goto T, Kang YJ, Maeda S, Yoshida H, Omata M, Asahara H, Koike K: Microrna-140 acts as a liver tumor suppressor by controlling nf-κb activity by directly targeting dna methyltransferase 1 (dnmt1) expression. Hepatology 2013;57:162-170.

45 Kojima K, Takata A, Vadnais C, Otsuka M, Yoshikawa T, Akanuma M, Kondo Y, Kang YJ, Kishikawa T, Kato N, Xie Z, Zhang WJ, Yoshida H, Omata M, Nepveu A, Koike K: Microrna122 is a key regulator of α-fetoprotein expression and influences the aggressiveness of hepatocellular carcinoma. Nat Commun 2011;2:338.

Cancer Cell
Article

# ER Stress Cooperates with Hypernutrition to Trigger TNF-Dependent Spontaneous HCC Development

Hayato Nakagawa,[1,5,8] Atsushi Umemura,[1,8] Koji Taniguchi,[1] Joan Font-Burgada,[1] Debanjan Dhar,[1] Hisanobu Ogata,[1,6] Zhenyu Zhong,[1] Mark A. Valasek,[2] Ekihiro Seki,[3] Juan Hidalgo,[4] Kazuhiko Koike,[5] Randal J. Kaufman,[7] and Michael Karin[1,2,*]

[1]Laboratory of Gene Regulation and Signal Transduction, Department of Pharmacology
[2]Department of Pathology
[3]Department of Medicine
School of Medicine, University of California, San Diego, 9500 Gilman Drive, San Diego, CA 92093, USA
[4]Department of Cell Biology, Physiology and Immunology, Institute of Neurosciences, Universitat Autonoma de Barcelona, Bellaterra, 08193 Barcelona, Spain
[5]Department of Gastroenterology, University of Tokyo, 7-3-1 Hongo, Bunkyo-ku, Tokyo 113-8655, Japan
[6]Department of Medicine and Clinical Science, Graduate School of Medical Sciences, Kyushu University, Fukuoka 812-8582, Japan
[7]Program in Degenerative Diseases, Sanford-Burnham Medical Research Institute, 10901 North Torrey Pines Road, La Jolla, CA 92037, USA
[8]Co-first author
*Correspondence: karinoffice@ucsd.edu
http://dx.doi.org/10.1016/j.ccr.2014.07.001

## SUMMARY

Endoplasmic reticulum (ER) stress has been implicated in the pathogenesis of viral hepatitis, insulin resistance, hepatosteatosis, and nonalcoholic steatohepatitis (NASH), disorders that increase risk of hepatocellular carcinoma (HCC). To determine whether and how ER stress contributes to obesity-driven hepatic tumorigenesis we fed wild-type (*WT*) and *MUP-uPA* mice, in which hepatocyte ER stress is induced by plasminogen activator expression, with high-fat diet. Although both strains were equally insulin resistant, the *MUP-uPA* mice exhibited more liver damage, more immune infiltration, and increased lipogenesis and, as a result, displayed classical NASH signs and developed typical steatohepatitic HCC. Both NASH and HCC development were dependent on TNF produced by inflammatory macrophages that accumulate in the *MUP-uPA* liver in response to hepatocyte ER stress.

## INTRODUCTION

Hepatocellular carcinoma (HCC) is the fifth most common cancer worldwide and a leading cause of cancer deaths. More than 90% of HCC develops in the context of chronic liver disease, with hepatitis B virus (HBV) or hepatitis C virus (HCV) infections being the main causes. However, 30%–40% of Western HCC patients do not exhibit viral infections (El-Serag, 2011). Most of these patients are obese with manifestations of the metabolic syndrome and suffer from nonalcoholic steatohepatitis (NASH), a severe form of nonalcoholic fatty-liver disease (NAFLD) (Cohen et al., 2011). Indeed, obesity increases male HCC risk by up to 4.5-fold (Calle et al., 2005) and also increases HCC risk in viral hepatitis (Chen et al., 2008). Because the prevalence of obesity has been increasing worldwide, its association with hepatocarcinogenesis has attracted much attention. In previous studies, we have shown that feeding mice exposed to the hepatic carcinogen diethylnitrosamine (DEN) with high-fat diet (HFD) strongly enhanced HCC development (Park et al., 2010). Although low-grade liver inflammation associated with tumor necrosis factor (TNF) and interleukin-6 (IL-6) expression contributes to obesity-promoted HCC development in this model, it should be noted that wild-type (*WT*) mice do not develop NASH, even after DEN administration and prolonged HFD feeding. It is therefore not clear whether the mechanism identified in DEN-treated mice has much bearing on NASH-driven human HCC (Toffanin et al., 2010).

### Significance

ER stress is often observed in cancer, but its role in tumorigenesis has not been explored. ER stress also occurs in premalignant liver diseases, including NASH, which progress to HCC, a highly aggressive and common cancer. Our work demonstrates that, when combined with hypernutrition, ER stress of liver parenchymal cells results in NASH-like disease that spontaneously progresses to HCC through an inflammatory mechanism dependent on TNF and IκB kinase signaling.

In considering possible mechanisms through which obesity may promote HCC development, we decided to study the potential contribution of ER stress because obesity (Hotamisligil, 2010; Ozcan et al., 2006) and HBV/HCV infections (Malhi and Kaufman, 2011) result in liver ER stress, which promotes hepatosteatosis (Rutkowski et al., 2008). Furthermore, several ER stress markers are elevated in NASH-affected livers (Puri et al., 2008), and it was suggested that ER stress causes ballooning degeneration of the hepatocytes, a classical sign of NASH (Caldwell et al., 2010). To this end, we placed *MUP-uPA* mice, which express high amounts of urokinase plasminogen activator (uPA) specifically in the hepatocytes and therefore undergo transient ER stress (Sandgren et al., 1991; Weglarz et al., 2000), and *WT* mice on a HFD. Whereas the *WT* mice developed simple steatosis and no HCC, the *MUP-uPA* mice developed NASH-like disease that spontaneously progressed to HCC, whose development was dependent on TNF production by inflammatory liver macrophages and TNF receptor 1 (TNFR1)-IκB kinase β (IKKβ) signaling in hepatocytes. Our results suggest that NASH and progression to steatohepatitic HCC may be prevented or ameliorated by anti-TNF drugs.

## RESULTS

### HFD Induces NASH Signs and Spontaneous HCC in *MUP-uPA* Mice

*WT* and *MUP-uPA* mice were placed on a HFD (60% of calories were fat derived), starting at 6 weeks of age. Body weight and glucose intolerance did not differ between the two strains (Figures S1A and S1B available online). As reported (Weglarz et al., 2000), the serum alanine aminotransferase (ALT) level in *MUP-uPA* mice on a normal-chow diet (low-fat diet [LFD]) was markedly elevated at 5 weeks of age but rapidly declined, probably due to the replacement of dying hepatocytes with new cells in which uPA expression was extinguished (Sandgren et al., 1991; Weglarz et al., 2000) (Figure S1C). However, HFD feeding maintained high serum ALT throughout the observation period (Figure 1A), even though it did not restore uPA expression (Figure S1C). By contrast, in *WT* mice the HFD substantially elevated the ALT after only 32 weeks, and it reached a level similar to *MUP-uPA* mice at 40 weeks. Examination of the liver histology revealed hepatocyte damage, evidenced by tissue clearing, in 5-week-old *MUP-uPA* mice, but this had almost disappeared at 24 weeks on the LFD, except for mild inflammation and spotty necrosis (Figure 1B). As reported (Park et al., 2010), HFD-fed *WT* mice showed pronounced steatosis but little inflammation by 24 weeks (Figure 1B). At that time, HFD-fed *MUP-uPA* mice exhibited extensive immune infiltration into the liver and numerous ballooning hepatocytes, both of which are important diagnostic features of human NASH (Brunt, 2001). Furthermore, HFD-fed *MUP-uPA* mice showed pericellular and bridging fibrosis, resembling the pattern in human NASH (Figure 1C; Figure S1D). This was accompanied by the increased expression of type 1 collagen α1 mRNA (Figure S1E).

Terminal deoxynucleotidyl transferase-mediated deoxyuridine triphosphate nick-end labeling (TUNEL) staining showed that both apoptotic (nuclear fragmentation) and necrotic (diffuse cytoplasmic staining) cell death were significantly increased in HFD-fed *MUP-uPA* livers and that, as a result, the numbers of Ki67-positive proliferating hepatocytes and K19-positive cells were also elevated (Figure 1D). The expression of cyclin D1 was also increased (Figure S1F). Thus, HFD-fed *MUP-uPA* mice exhibit continuous hepatocyte death and compensatory proliferation, a critical process in hepatocarcinogenesis (Maeda et al., 2005).

HFD-fed *MUP-uPA* mice developed small tumors on the liver surface by 32 weeks of age and large tumors at 40 weeks (Figure 2A; Figures S2A and S2B), when 78.6% (11/14 mice) of HFD-fed *MUP-uPA* mice had tumors larger than 2 mm and 35.7% (5/14 mice) had tumors larger than 10 mm. Histologically, 30% of tumors larger than 2 mm were HCCs, similar to human steatohepatitic HCC, a histotype describing NASH-related HCC with ballooning cancer cells and inflammatory cell infiltration (Salomao et al., 2012), although some displayed a classical thick trabecular pattern, whereas the remaining 70% were either typical or steatohepatic adenomas (Figure 2B; Figures S2C and S2D). Cancer cells were highly proliferative and frequently positive for α fetoprotein (AFP) with marked p62 aggregation (Figure S2E), a sign of impaired autophagy frequently observed in human HCC (Inami et al., 2011). Several oncogenic mediators, such as extracellular signal regulated-kinase (ERK), signal transducer and activator of transcription 3 (STAT3), and c-Jun N-terminal kinase (JNK), as well as cyclin D1, the liver oncogenes Yes-associated protein 1 (YAP) and Myc, and the cancer stem cell markers epithelial cellular adhesion molecule (EpCAM) and CD44, were activated or upregulated (Figures S2F–S2H). By contrast, 30% of LFD-fed *MUP-uPA* mice displayed a few tiny nodules in the liver even at 40 weeks of age, corresponding to simple hyperplasia (Figure S2C). Although 1 of 11 LFD-fed *MUP-uPA* mice developed a small 3 mm tumor, the tumor was also classified as hyperplasia, which is not proliferative and is AFP negative (Figures S2C and S2I). In *WT* mice, neither the LFD nor HFD induced any liver tumors by 40 weeks. Of note, HFD-fed *MUP-uPA* mice showed microscopically visible foci of p62- and YAP-positive cells already at 24 weeks (Figure S2J). These foci may contain progenitors to the tumors detected at 32–40 weeks. Thus, HFD feeding of *MUP-uPA* mice induced complete NASH-like pathological features with continuous hepatocyte death and compensatory proliferation, and eventually led to spontaneous HCC and adenoma development, which were not seen in the LFD-maintained mice.

### ER Stress Enhances Lipogenesis and Aggravates Steatohepatitis

Although the mechanism responsible for hepatocyte death in young *MUP-uPA* mice is not entirely clear, their hepatocytes are ER stressed (Sandgren et al., 1991). Indeed, several ER stress markers, including C/EBP homologous protein (CHOP), glucose-regulated protein 78 (GRP78), spliced X-box binding protein 1 (sXBP1), phosphorylated eIF2α (p-eIF2α), phosphorylated inositol-requiring enzyme 1α (p-IRE1α), and phosphorylated JNK (p-JNK), were elevated in 5-week-old *MUP-uPA* mice compared to *WT* (Figure 3A; Figure S3A). Whereas in 16-week-old *MUP-uPA* mice most markers declined, paralleling the decline in uPA expression, HFD-fed *MUP-uPA* mice maintained strong eIF2α and JNK phosphorylation and CHOP expression (Figure 3B; Figure S3A). In *WT* mice, HFD feeding induced only a slight elevation in p-eIF2α and CHOP mRNA, with no effect on CHOP protein (Figure 3B). Using

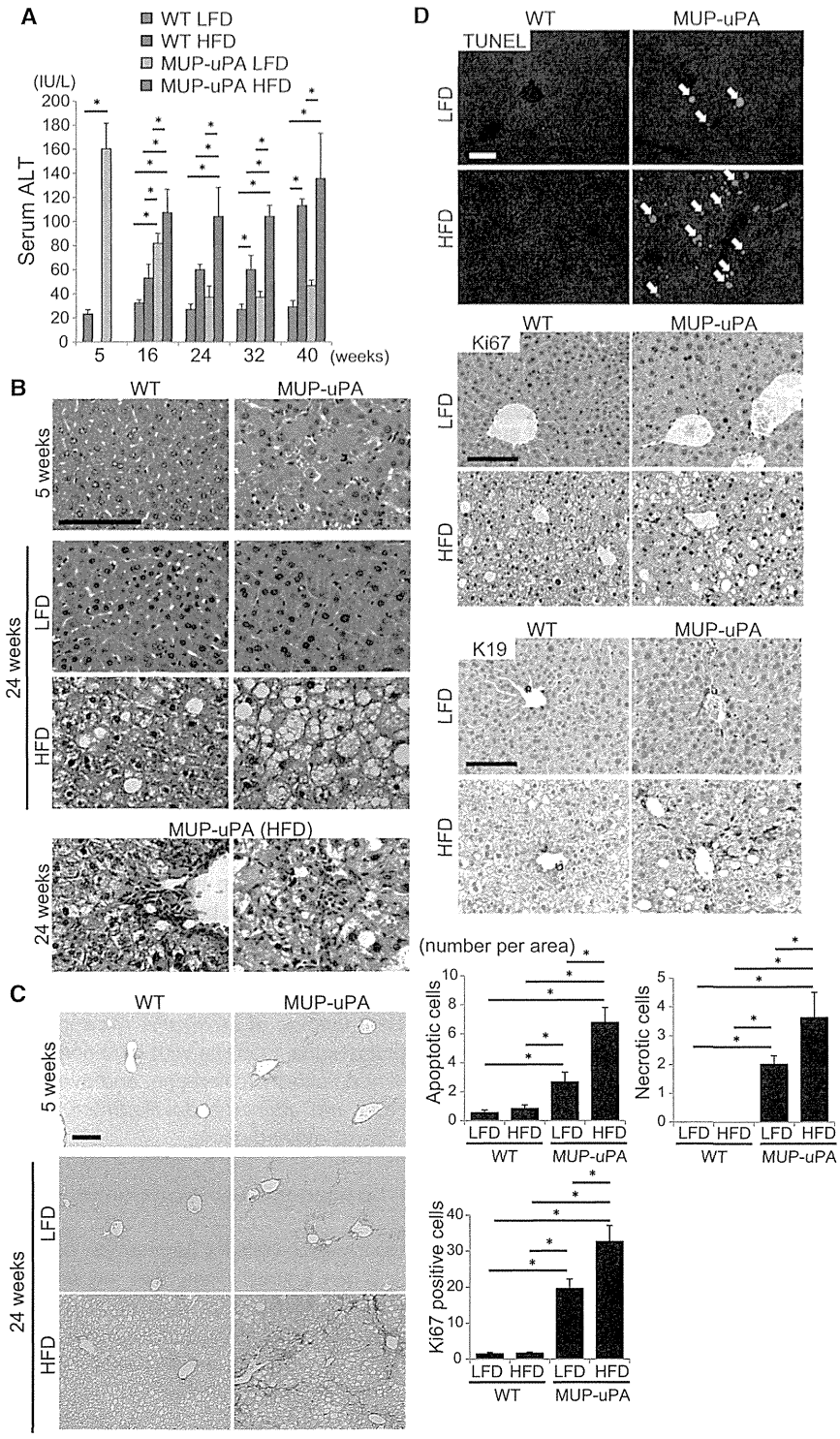


**Figure 1. HFD-Fed *MUP-uPA* Mice Display Classical NASH Signs**

(A) Serum ALT in LFD- or HFD-fed *WT* and *MUP-uPA* mice was measured at indicated ages. HFD feeding was initiated at 6 weeks. Data are means ± SD (n = 3–5 per group). *p < 0.05.

(B) H&E staining of liver sections from 5-week-old mice on the LFD and 24-week-old mice kept on the LFD or HFD (scale bar, 100 μm). The bottom two panels show the infiltration of immune cells in HFD-fed *MUP-uPA* mouse livers (left, portal area; right, liver parenchyma).

(C) Sirius Red staining of liver sections described in (B) (scale bar, 100 μm).

(D) TUNEL and IHC analyses of Ki67 and K19 in 24-week-old mice that were kept on the LFD or HFD (scale bar, 100 μm). Yellow and white arrows indicate apoptotic and necrotic cells, respectively. Bar graphs show the numbers of apoptotic and necrotic cells and Ki67-positive cells per 200X field. Data are means ± SD (n = 5 per group). *p < 0.05.

See also Figure S1.

immunohistochemistry (IHC), we confirmed the level of nuclear CHOP in the hepatocytes of 5-week-old *MUP-uPA* mice, which was sustained at 16 weeks of age only in the HFD-fed *MUP-uPA* mice (Figure 3C). Tribble3 (TRB3) and death receptor 5 (DR5), two molecules capable of inducing cell death, were highly upregulated in *MUP-uPA* mice, especially after HFD feeding (Figure S3B). After 24 weeks of the HFD, expression of the DR5 ligand TNF-related apoptosis-inducing ligand (TRAIL) was also elevated in the *MUP-uPA* liver. Electron microscopy (EM) revealed distended and dilated ERs in HFD-fed *MUP-uPA* mice (Figure S3C). Thus, whereas ER stress appears to be induced by uPA expression in 5-week-old *MUP-uPA* mice, it declines due to transgene extinction. However, feeding these mice with HFD rekindles the stress response and induces several cell-death mediators that are not expressed in HFD-fed *WT* mice. To determine whether ER stress can cause ballooning degeneration and hepatocyte death, we injected HFD-fed *WT* mice with the protein-glycosylation inhibitor and ER-stress elicitor tunicamycin. This treatment led to rapid (36 hr) induction of ballooning degeneration, hepatocyte apoptosis, and ALT release only in the HFD-fed mice (Figures S3D–S3F). The white appearance of the liver from HFD-fed mice treated with tunicamycin suggested that the liver had become more steatotic.

These results are consistent with the ability of ER stress to cause liver steatosis (Rutkowski et al., 2008). Indeed, Oil Red O (ORO) staining showed mild spontaneous lipid accumulation in 5-week-old *MUP-uPA* mice, which diminished by 16 weeks of age under the LFD (Figure 3D). However, HFD feeding induced more extensive lipid accumulation in the *MUP-uPA* than in the *WT* mice. Liver triglycerides (TGs) and cholesterol were also elevated (Figure 3E). Decreased liver lipid export due to the suppression of apolipoprotein B (apoB) expression/secretion and increased lipogenesis were suggested

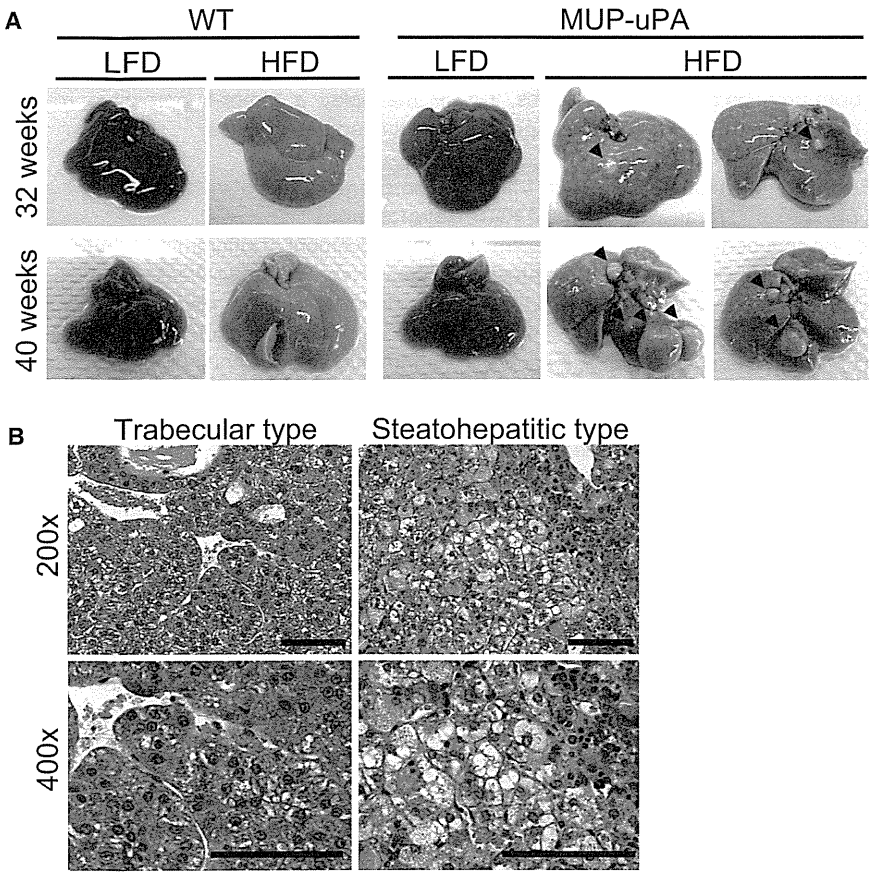


**Figure 2. NASH to HCC Progression in *MUP-uPA* Mice**

(A) Representative images of livers from 32- and 40-week-old mice that were kept on the LFD or HFD.

(B) Representative H&E staining of tumor sections from 40-week-old HFD-fed *MUP-uPA* mice. The left two panels show trabecular HCC, and the right two panels show steatohepatitic HCC (scale bar, 100 μm).

See also Figure S2.

to be involved in ER stress-induced steatosis (Ota et al., 2008; Qiu et al., 2011; Rutkowski et al., 2008). Because apoB carries TGs and cholesterol from the liver elsewhere, we examined serum TGs and cholesterol and liver apoB mRNA. There were no differences in apoB mRNA among the four groups (Figure S3G), and the serum TGs and total cholesterol were similarly elevated in HFD-fed *WT* and *MUP-uPA* mice (Figure S3H), suggesting that liver lipid export was not fully impaired in *MUP-uPA* mice. Next, we examined the mRNAs of lipogenic regulators. Although sterol regulatory element-binding protein 2 (SREBP2) mRNA was slightly increased and peroxisome proliferator-activated receptor α (PPARα) and CCAAT/enhancer-binding protein α (c/EBPα) mRNAs were slightly decreased in the 5-week-old *MUP-uPA* mice compared to the *WT* mice, these trends were not seen in the 16-week-old mice (Figure S3I). Expression of PPARγ was decreased in the 16-week-old *MUP-uPA* mice but not in the 5-week-old mice. Therefore, the enhanced lipogenesis in *MUP-uPA* mice could not be explained by the differential expression of these molecules. However, among lipogenic regulators, SREBP1 is controlled not only by synthesis but also by cleavage and subsequent nuclear translocation (Goldstein et al., 2006), which are stimulated by ER stress (Kammoun et al., 2009). Indeed, the SREBP1 precursor abundance was decreased in the 5-week-old *MUP-uPA* livers, and mature nuclear SREBP1 was elevated (Figure 3F). HFD feeding further accelerated SREBP1 processing in the *MUP-uPA* mice but also induced some SREBP1 processing in the *WT* mice. The mRNA expression of the SREBP1 target fatty-acid synthase (FAS), was increased in the 5-week-old and HFD-fed *MUP-uPA* mice (Figure 3G). Consistent with elevated lipogenesis, gas chromatography determination of the hepatic fatty-acid (FA) composition revealed a significant increase in C16:0 palmitic acid (PA) and longer-chain FA in *MUP-uPA* mice compared to *WT* mice, which was further enhanced by HFD feeding (Figure 3H). Excess lipid accumulation leads to oxidative stress due to mitochondrial $H_2O_2$ production, which can induce cell death (Anderson et al., 2009). Accordingly, the HFD-fed *MUP-uPA* mice displayed strong dihydroethidium (DHE) staining of hepatocytes and a decrease in liver reduced glutathione (GSH): oxidized glutathione (GSSG) ratio (Figures 3I and 3J). Oxidative stress in HFD-fed *MUP-uPA* mice may contribute to CHOP expression, JNK activation, lipotoxic hepatocyte death, and oncogenic mutations.

The IRE1α-XBP1 pathway has been reported to regulate the hepatic lipid metabolism via the XBP1-mediated induction of lipogenic enzymes and regulated IRE1-dependent mRNA decay (RIDD) (Lee et al., 2008; So et al., 2012). Although expression of the XBP1 target gene ERdj4 was upregulated in the 5-week-old and HFD-fed *MUP-uPA* mice, there were no differences in expression of diacylglycerol O-acyltransferase 2, a lipogenic enzyme regulated by XBP1 but not by SREBP1 (Figure S3J). RIDD-mediated downregulation of angiopoietein-like protein 3 (Angptl3) and carboxylesterase 1 (Ces1) mRNAs can induce hypolipidemia and hepatosteatosis due to decreased lipid secretion from the liver. Although expression of Angptl3 mRNA was decreased in 5-week-old *MUP-uPA* mice (Figure S3J), there were no differences in serum TGs and total cholesterol levels between the 5-week-old *WT* and *MUP-uPA* mice and in Angptl3 mRNA expression recovered in 16-week-old *MUP-uPA* mice (Figures S3H and S3J). These results suggest that the IRE1-α-XBP1 pathway does not play a major role in NASH development in *MUP-uPA* mice.

### Chemical Chaperons and GRP78 Attenuate Lipotoxicity and Lipogenesis in *MUP-uPA* Mice

To examine whether ER stress enhances lipotoxicity in *MUP-uPA* hepatocytes, we incubated *WT* and *MUP-uPA* hepatocytes with PA. After 24 hr, lipotoxic cell death was seen in both *WT* and

*MUP-uPA* hepatocytes but was more extensive in the latter (Figure 4A). PA increased CHOP expression and SREBP1 maturation in *WT* hepatocytes, but these effects were more pronounced in *MUP-uPA* hepatocytes, which expressed both proteins prior to PA addition (Figure 4B). To examine the contribution of ER stress to these phenomena, we treated hepatocytes with the chemical chaperons 4-phenylbutyrate (4-PBA) and tauro-ursodeoxycholic acid (TUDCA), which reduce ER stress (Ozcan et al., 2006). Both compounds attenuated PA-induced cell death, but their prosurvival effect was more pronounced in *MUP-uPA* hepatocytes (Figure 4A). CHOP induction and SREBP1 maturation upon PA treatment were also reduced by 4-PBA (Figure 4B). Overexpression of the ER protein chaperon GRP78 in *MUP-uPA* hepatocytes also inhibited SREBP1 maturation and PA-induced cell death (Figures 4C and 4D), further supporting the role of ER stress in both phenomena. PA treatment activated JNK, but consistent with previous results that ER stress has only a partial role in JNK activation by PA (Holzer et al., 2011), the effect was restricted to *WT* hepatocytes and 4-PBA treatment only partially reduced JNK phosphorylation (Figure 4B). Nonetheless, the JNK inhibitor D-JNKi protected both cell types from PA-induced death (Figure 4E).

We examined the effect of TUDCA on NASH development. We initiated daily intraperitoneal (i.p.) injections of TUDCA (250 mg/kg) or phosphate-buffered saline (PBS; vehicle control) to the HFD-fed *MUP-uPA* mice at 16 weeks of age. After 4 weeks, hepatosteatosis and hepatocyte ballooning were attenuated (Figure 4F) and serum ALT and hepatic TGs and cholesterol were significantly reduced (Figures 4G–4I). Hepatocyte death and reactive oxygen species (ROS) accumulation were also suppressed (Figures S4A and S4B). TUDCA treatment also inhibited CHOP expression and SREBP1 maturation in livers of the HFD-fed *MUP-uPA* mice (Figure S4C). We also found that in vivo overexpression of GRP78 using an adenovirus vector attenuated hepatic steatosis in the HFD-fed *MUP-uPA* mice (Figures S4D and S4E). However, due to enhanced adenovirus toxicity in *MUP-uPA* mice, we could not assess the effect on NASH and HCC development. Nonetheless, the results suggest that increased lipotoxicity caused by a positively reinforced cycle of ER stress, oxidative stress, and lipogenesis aggravates fatty liver disease in HFD-fed *MUP-uPA* mice.

Given the pronounced expression of CHOP in *MUP-uPA* mice and its postulated role in apoptosis (Malhi and Kaufman, 2011), we crossed *MUP-uPA* mice to $Chop^{\Delta hep}$ mice, in which CHOP was deleted in hepatocytes. Despite efficient CHOP ablation, there was no reduction in liver damage, JNK and eIF2$\alpha$ phosphorylation, or GRP78 expression in young $Chop^{\Delta hep}$/*MUP-uPA* mice (Figures S4F and S4G). Correspondingly, CHOP ablation did not inhibit HCC development (Figure S4H). In fact, CHOP ablation increased tumor multiplicity without affecting tumor size, ER stress markers, or NASH severity (Figures S4I–S4K), results that stand in marked contrast to the protective effect of whole-body *Chop* ablation in DEN-induced hepatocarcinogenesis (DeZwaan-McCabe et al., 2013). CHOP was strongly expressed in some tumors and preneoplastic lesions of HFD-fed *MUP-uPA* mice but not in $Chop^{\Delta hep}$/*MUP-uPA* mice, and the number of TUNEL-positive cells tended to be reduced in the tumor tissues of $Chop^{\Delta hep}$/*MUP-uPA* mice (Figures S4L and S4M), suggesting that hepatocyte CHOP is not positively involved in NASH progression and HCC development, similar to what was observed in whole-body $Chop^{-/-}$ mice on a methionine-choline-deficient (MCD) diet (Soon et al., 2010). Nonetheless, CHOP may play a tumor-suppressive role by inducing apoptosis of initiated hepatocytes.

### TNF from Liver Macrophages Promotes Lipogenesis and NASH and HCC Development

Next, we examined the involvement of inflammatory cytokines in hepatosteatosis and steatohepatitis. In 24-week-old mice, TNF and IL-1$\beta$, but not IL-6, mRNAs were elevated in HFD-fed *MUP-uPA* livers (Figure 5A). TNF production was confirmed by ELISA (Figure 5B) and immunofluorescence (IF) analysis localized it to F4/80-positive macrophages, whose number was elevated in HFD-fed *MUP-uPA* mouse livers (Figure 5C). The increase in macrophage infiltration and TNF expression was inhibited by TUDCA treatment (Figures S5A and S5B), suggesting that it is stimulated, in part, by hepatocyte ER and oxidative stress.

To investigate the role of TNF in NASH progression and HCC development, we generated TNF receptor 1 (TNFR1)-deficient *MUP-uPA* ($Tnfr1^{-/-}$/*MUP-uPA*) mice. At 5 and 40 weeks of age, there were no differences in liver injury and body weights between the *MUP-uPA* and $Tnfr1^{-/-}$/*MUP-uPA* mice (Figures S5C–S5F). We placed these mice on the HFD from 6 to 40 weeks of age, and assessed the liver histology and tumorigenesis. Body-weight gain at 40 weeks of age was similar between *MUP-uPA* and $Tnfr1^{-/-}$/*MUP-uPA* mice (Figure S5F), but tumor development was substantially reduced upon TNFR1 ablation (Figures 5D and 5E). Importantly, hepatocyte ballooning, ALT release, liver TGs, and cholesterol, as well as SREBP1 and JNK activation, were reduced in the $Tnfr1^{-/-}$/*MUP-uPA* mice (Figures 5F–5I). Therefore, TNFR1 signaling perpetuates NASH pathogenesis and HCC progression.

### TNFR1 Signaling Directly Promotes Tumor Growth

To determine whether TNFR1 signaling promotes HCC development by acting in HCC progenitor cells (HcPCs), whose isolation we recently described (He et al., 2013), we transplanted HcPCs from DEN-treated *WT* or $Tnfr1^{-/-}$ mice into *MUP-uPA* mice, which were placed on the LFD or HFD (Figure 6A). The expression of the HcPC marker CD44 was comparable between *WT* and $Tnfr1^{-/-}$ HcPCs (Figure S6A). After 5 months, nontransplanted *MUP-uPA* mice did not have any tumors larger than 2 mm, even after HFD feeding, whereas HcPC-transplanted mice developed multiple HCC nodules (Figure 6B). The HFD feeding did not affect the number of tumors (which was determined by the number of transplanted HcPCs); however, it significantly increased the tumor size in mice transplanted with *WT* HcPCs but not in mice receiving $Tnfr1^{-/-}$ HcPCs (Figures 6B and 6C). Thus, although TNFR1 signaling is dispensable for HcPC induction by DEN, it strongly stimulates tumor growth in a cell-autonomous manner. Control experiments confirmed that TNFR1 was deleted in HCC cells but not in nontumor liver tissues (Figure S6B). In addition, there were no differences in NASH-like pathology and TNF expression in the background liver harboring either *WT* or $Tnfr1^{-/-}$ HcPCs (Figures S6C–S6G). To further investigate the role of TNF signaling in these effects, we treated *WT* HcPC-transplanted *MUP-uPA* mice with the TNF antagonist etanercept

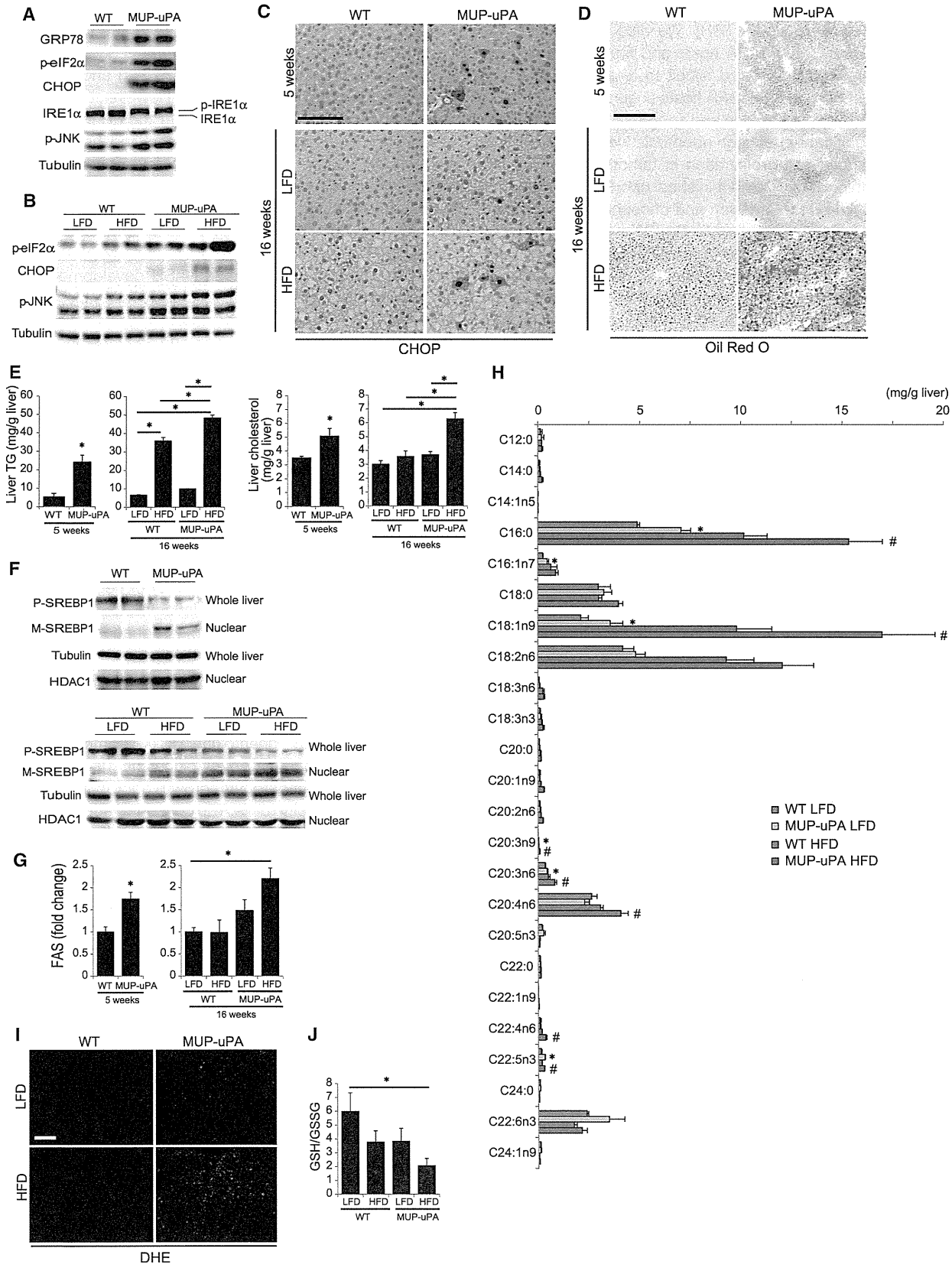


(legend on next page)

under HFD feeding. Etanercept treatment significantly suppressed HCC growth (Figure S6H). We also transplanted *WT* HcPCs into *Tnfr1*$^{-/-}$*/MUP-uPA* hosts and found that the HFD still led to increased tumor size, albeit to a lesser extent than the 2-fold effect seen in *MUP-uPA* hosts (Figure S6I).

We assessed cell proliferation and apoptosis in HcPC-derived tumors. No significant effects on apoptosis were observed, but the HFD enhanced cell proliferation in tumors formed by *WT* HcPCs, and this effect was diminished upon TNFR1 ablation (Figure 6D). Cyclin D1 expression and phosphorylation of ERK, STAT3, JNK, and ribosomal protein S6 (S6) were enhanced by HFD feeding in *WT* HcPC-derived tumors (Figure 6E; Figure S6J). Apart from S6 phosphorylation, these responses were abolished upon TNFR1 ablation. TNFR1 in HcPCs was also required for nuclear factor κ B (NF-κB) activation in tumors that developed in HFD-fed *MUP-uPA* mice (Figure 6F) and IKKβ ablation in HcPC prevented, HFD-enhanced tumor growth (Figure 6G). Thus the TNF-TNFR1-IKKβ-NF-κB pathway is an important mediator of HCC growth in HFD-fed mice.

### TNFR1 Signaling Promotes Tumor-Associated Inflammation

Some of the signaling effectors that are activated in HFD-fed mice are not directly regulated by TNFR1. We postulated that autocrine or paracrine signaling may mediate some of the observed responses and analyzed tumors generated by *WT* and *Tnfr1*$^{-/-}$ HcPCs more closely. In HFD-fed mice, both *WT* and *Tnfr1*$^{-/-}$ HCCs were composed of steatotic cells, but immune infiltration was less extensive in *Tnfr1*$^{-/-}$ HCCs (Figure 7A). Real-time PCR and IHC analysis indicated that macrophage and B cell markers were significantly increased by the HFD in *WT* but not in *Tnfr1*$^{-/-}$ HCCs (Figures 7B and 7C). In addition, mRNAs for numerous inflammatory cytokines, chemokines, and growth factors were upregulated by the HFD in *WT* but not in *Tnfr1*$^{-/-}$ HCCs (Figure S7). IF analysis confirmed that expression of chemokine (C-C motif) ligand 7 (CCL7), which attracts macrophages and monocytes, was increased by the HFD in *WT* but not in *Tnfr1*$^{-/-}$ HCCs (Figure 7D). Thus, TNFR1 signaling in HCC cells promotes tumor-associated inflammation, which can account for ERK and STAT3 activation in malignant cells.

## DISCUSSION

ER stress and the unfolded protein response (UPR) are upregulated in many cancers and may be associated with drug resistance and adaptation to the transformed state (Wang et al., 2010). Elevated ER stress was also detected in precancerous conditions that precede HCC development, including HBV and HCV infections (Malhi and Kaufman, 2011) and NASH (Farrell et al., 2012; Tilg and Moschen, 2010). However, until recently, researchers have not examined whether the ER stress response, which contributes to insulin resistance and hepatic steatosis (Hotamisligil, 2010), stimulates HCC development. Our results indicate that transient ER stress does not trigger hepatocarcinogenesis in *MUP-uPA* mice that are kept on a LFD but that it elicits a more sustained stress response that also includes extensive oxidative stress when combined with hypernutrition. This response leads to spontaneous NASH development and progression to HCC, whose features closely resemble steatohepatitic HCC in NASH patients. Our studies suggest several potential mechanisms related to ER stress and HFD feeding that cooperate to induce HCC development. First, by stimulating hepatosteatosis (lipid droplet accumulation), HFD sustains a modest degree of ER stress in *MUP-uPA* mice, which otherwise would be switched off upon extinction of uPA expression. Second, ER stress promotes SREBP1 activation, enhancing lipogenesis and increasing the degree of hepatic steatosis beyond what is achieved by HFD alone. Third, ER stress and steatosis increase ROS production in hepatocytes to cause oxidative stress and its sequelae, which include genomic instability, oncogenic mutations, and/or gene-copy-number changes. Fourth, ER and oxidative stress increase the sensitivity of hepatocytes to lipotoxic death, thereby releasing inflammatory mediators that attract and activate monocytes/macrophages. Fifth, TNF and other mediators produced by activated inflammatory macrophages stimulate compensatory hepatocyte proliferation and expand HCC progenitors. TNF further reinforces the inflammatory microenvironment and induces expression of chemokines (CCL2, CCL7, and chemokine [C-X-C motif] ligand 13 [CXCL13]) and growth factors/cytokines (IL-1β, IL-6, TNF itself, lymphotoxin, and hepatocyte growth factor [HGF]) both by HcPCs and surrounding cells. The concerted action of these factors contributes to the development of NASH-like pathology, and NASH contributes to HCC progression. Mutually reinforcing ER stress and hepatosteatosis (Malhi and Kaufman, 2011) are needed to set this pathogenic cascade in motion.

The requirement for two hits (hepatosteatosis and ER stress) for the induction of HCC development in *MUP-uPA* mice resembles that which has been proposed to drive NASH development, a pre-HCC condition, in humans (Day and James, 1998; Tilg and

**Figure 3. ER Stress Enhances Lipogenesis and Promotes Steatohepatitis**

(A and B) Immunoblot (IB) analysis of ER stress markers in livers of 5-week-old *WT* and *MUP-uPA* mice (A) and 16-week-old *WT* and *MUP-uPA* mice kept on the LFD or HFD (B).

(C) IHC analysis of CHOP in livers of 5-week-old mice on the LFD and 16-week-old mice kept on the LFD or HFD (scale bar, 100 μm).

(D) Oil Red O staining of mouse livers described in (C) (scale bar, 100 μm).

(E) TG and cholesterol content of mouse livers described in (C).

(F) IB analysis of unprocessed precursor SREBP1 (P-SREBP1) in whole liver extract and mature SREBP1 (M-SREBP1) in liver nuclei of mice described in (A) (upper panels) and (B) (lower panels).

(G) Real-time PCR analysis of liver FAS mRNA.

(H) Hepatic FA composition in 16-week-old mice kept on the LFD or HFD, analyzed using gas chromatography. *$p < 0.05$, compared with LFD-fed *WT* mice. #$p < 0.05$, compared with HFD-fed *WT* mice.

(I and J) ROS accumulation in 16-week-old mice that were kept on the LFD or HFD. Images of DHE staining (scale bar, 100 μm) (I) and GSH:GSSG ratio (J) are shown. All bar graphs represent means ± SD ($n = 3$ per group). *$p < 0.05$.

See also Figure S3.

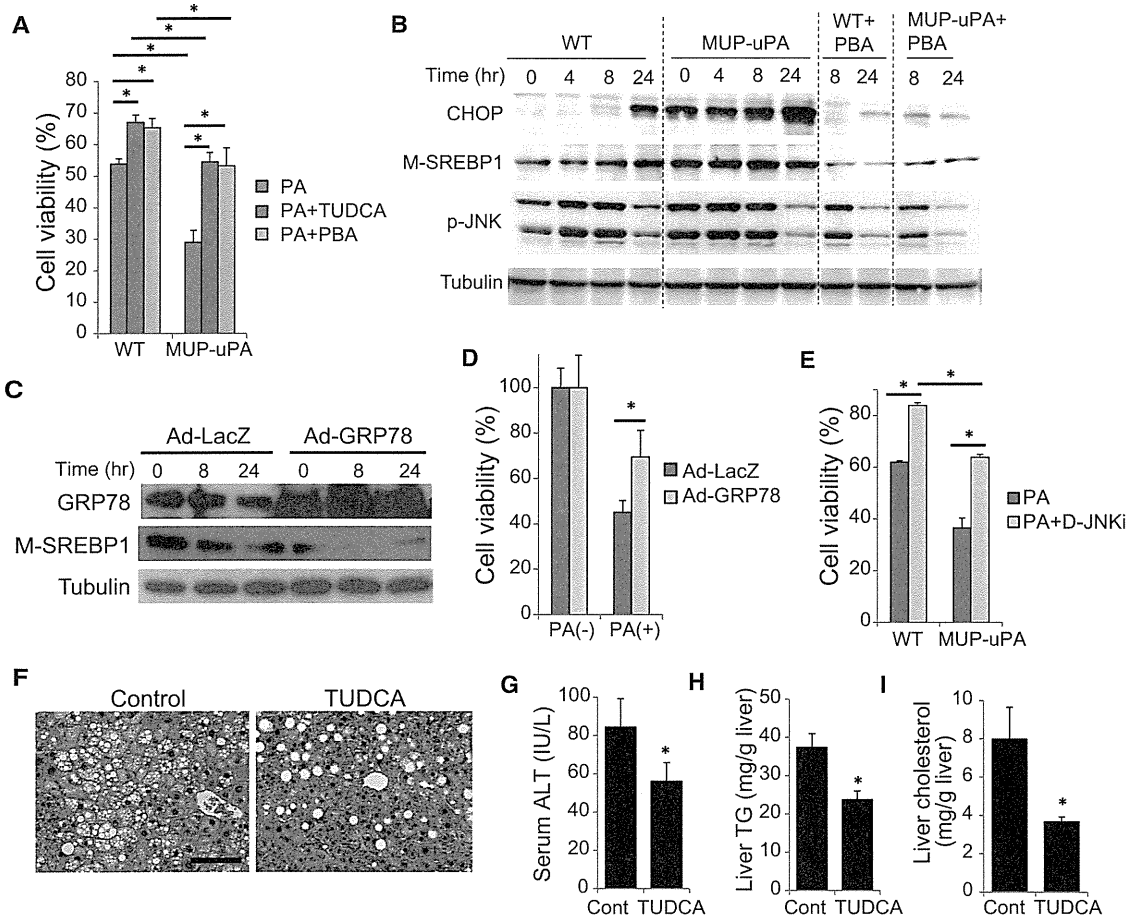


**Figure 4. Chemical Chaperons Attenuate Lipotoxicity and Liver Damage in *MUP-uPA* Mice**

(A) Primary hepatocytes from *WT* and *MUP-uPA* mice were incubated with 300 μM PA for 24 hr with or without 500 μM TUDCA or 1 mM 4-PBA. Cell viability was assessed using Cell Counting Kit-8 assay. Data are means ± SD of triplicate wells. *p < 0.05.

(B) Primary hepatocytes from *WT* and *MUP-uPA* mice were incubated with 200 μM PA with or without 4-PBA as in (A). CHOP expression, SREBP1 maturation, and JNK phosphorylation were assessed using IB.

(C and D) Effect of GRP78 overexpression. *MUP-uPA* hepatocytes were infected with adenoviruses encoding LacZ or GRP78 and then incubated with PA. SREBP1 maturation (C) and cell viability (D) were assessed as in (B).

(E) Hepatocytes from *WT* and *MUP-uPA* mice were incubated with 300 μM PA for 24 hr with or without 10 μM D-JNKi, and cell viability was assessed. Data are means ± SD of triplicate wells. *p < 0.05.

(F–I) Effect of TUDCA on NASH in HFD-fed *MUP-uPA* mice. The 16-week-old HFD-fed *MUP-uPA* mice were i.p. injected with TUDCA (250 mg/kg) or the vehicle, and after 4 weeks of daily treatment, liver histology (scale bar, 100 μm) (F), serum ALT (G), liver TGs (H), and liver cholesterol (I) were evaluated. Bar graphs are means ± SD (n = 5 per group). *p < 0.05.

See also Figure S4.

Moschen, 2010). Although simple steatosis (not NASH) is an extremely common disorder affecting nearly 30% of the US population, only 10%–20% of these patients develop NASH. In the absence of known genetic factors, it was proposed that NASH development depends on multiple secondary hits, which may include microbiota-related factors, food additives, dysbiosis, IL-6 and TNF from adipose tissue, mitochondrial dysfunction, and oxidative or ER stress (Farrell et al., 2012; Tilg and Moschen, 2010). Although these are considered secondary hits, they may act as pre-existing risk factors prior to hepatosteatosis caused by a HFD. Nonetheless, in humans, unlike *MUP-uPA* mice, it has been extremely difficult to detect the presence of such risk factors because they do not lead to overt liver damage (elevated ALT) prior to development of a steatotic liver due to hypernutrition. Given its presence in other pre-HCC conditions (Malhi and Kaufman, 2011), we focused our study on the role of ER stress. Remarkably, feeding a HFD to *MUP-uPA* mice resulted in steatohepatitis that closely resembled human NASH, and two of the main pathological features, ballooning degeneration and hepatocyte death, were also rapidly induced by the administration of tunicamycin to HFD-fed mice. By itself, short-term administration of tunicamycin did not damage the liver, but due to toxicity that may be associated with long-term use, we did not examine whether tunicamycin induces NASH and HCC in HFD-fed *WT* mice. Notably, NASH-like disease in *MUP-uPA* mice is associated with the same metabolic alterations linked

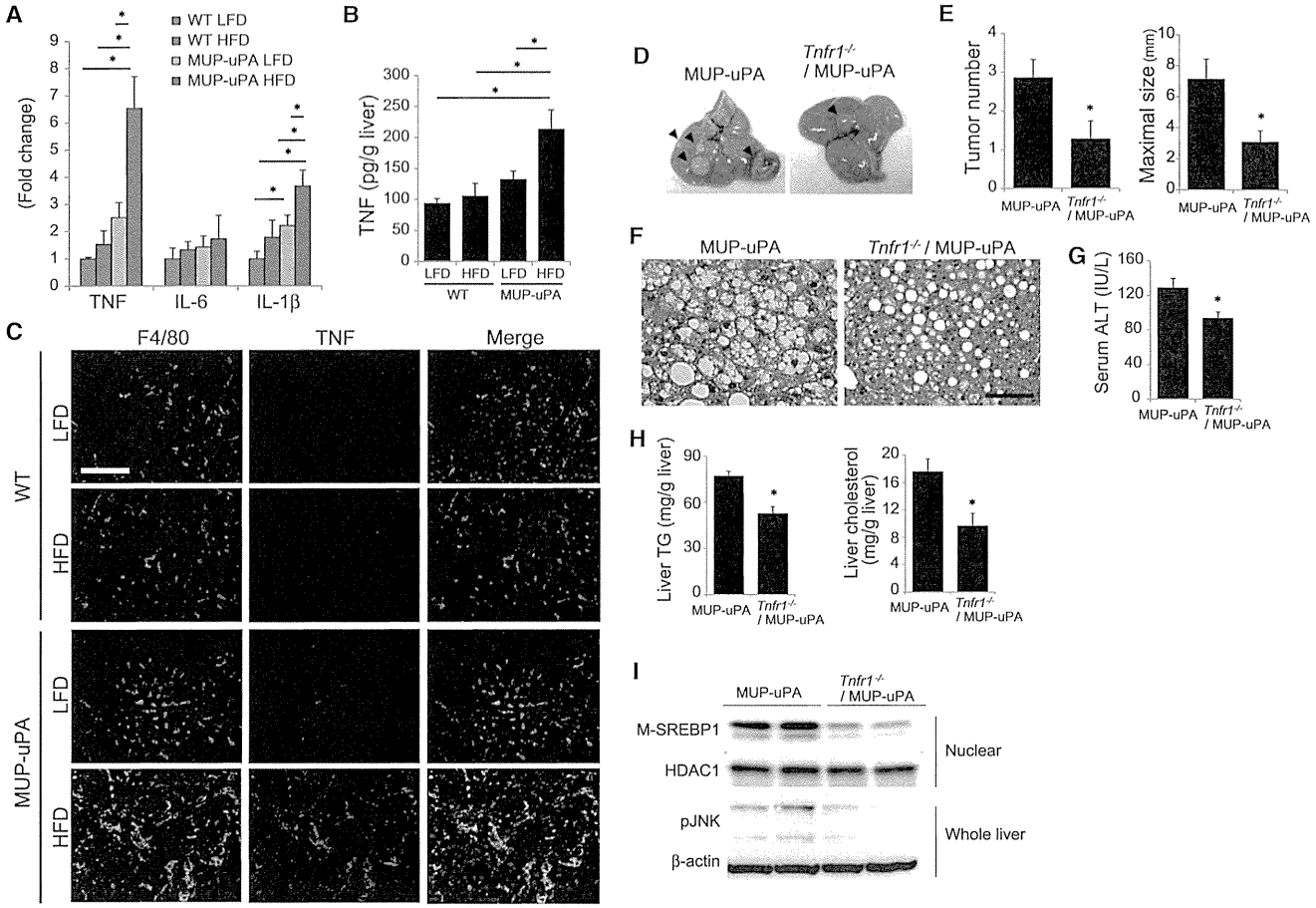


**Figure 5. TNFR1 Signaling Promotes Tumor Growth**

(A) Relative inflammatory cytokine mRNA in livers of 24-week-old mice kept on the LFD or HFD determined by real-time qPCR. Data are means ± SD (LFD-fed *WT*, n = 3; others, n = 5 per group). *p < 0.05.

(B) TNF protein in livers from (A) was measured using ELISA. Data are means ± SD. *p < 0.05.

(C) Double IF analysis of F4/80 (green) and TNF (red) of liver sections from (A) (scale bar, 100 μm). Nuclei were labeled with DAPI (blue).

(D–G) Effect of TNFR1 ablation on NASH and tumorigenesis in HFD-fed *MUP-uPA* mice. *MUP-uPA* and *Tnfr1*$^{-/-}$*/MUP-uPA* mice were fed the HFD from 6 to 40 weeks of age. Representative images of livers (D), tumor numbers and maximal sizes (E), H&E staining of nontumor areas (scale bar, 100 μm) (F), and serum ALT (G) are shown. Bar graphs represent means ± SEM (*MUP-uPA*, n = 14; *Tnfr1*$^{-/-}$*/MUP-uPA*, n = 11). *p < 0.05.

(H) TG and cholesterol content in nontumor tissue of HFD-fed *MUP-uPA* and *Tnfr1*$^{-/-}$*/MUP-uPA* mouse livers. Bar graphs represent means ± SD (n = 7 per group). *p < 0.05.

(I) IB analyses showing effects of TNFR1 ablation on SREBP1 maturation and JNK phosphorylation in nontumor tissue of HFD-fed *MUP-uPA* mice.

See also Figure S5.

to NASH in humans and is not accompanied by weight loss, as seen in other NASH models that are based on feeding mice toxic diets that induce liver damage (Farrell et al., 2012). Furthermore, the HFD-fed *MUP-uPA* mouse is currently the only model for studying obesity-induced HCC development that does not rely on the administration of liver toxins or carcinogens. The major NASH-promoting effects of ER stress in this system are increased lipogenesis, oxidative stress, and susceptibility to lipotoxic cell death. ER stress contributes to SREBP activation, thereby stimulating lipogenesis (Kammoun et al., 2009). ER and oxidative stress also upregulate several cell-death mediators, including TRB3 and DR5, but the exact mechanisms through which ER stress promotes cell death remain controversial (Xu et al., 2005) and our results indicate that in normal hepatocytes it is CHOP independent. Although ER stress causes insulin resistance (Hotamisligil, 2010; Ozcan et al., 2006) and insulin resistance was proposed to contribute to HCC development, our results suggest that insulin resistance has no obvious role in HCC development because it is not higher in *MUP-uPA* mice than in HFD-fed *WT* mice.

A consequence of ER stress and lipotoxic hepatocyte death that contributes to HCC development is induction of TNF-dependent steatohepatitis. In addition to amplifying liver inflammation and shaping the inflammatory microenvironment near HcPC clusters, TNF contributes to hepatosteatosis and liver damage. Although TNFR1 engagement can trigger apoptosis, it is not responsible for ER-stress-induced death in lean *MUP-uPA* mice, and its contribution to liver damage in HFD-fed mice is proportional to its effect on lipogenesis and may be indirect. TNF, however, directly stimulates HCC growth through NF-κB

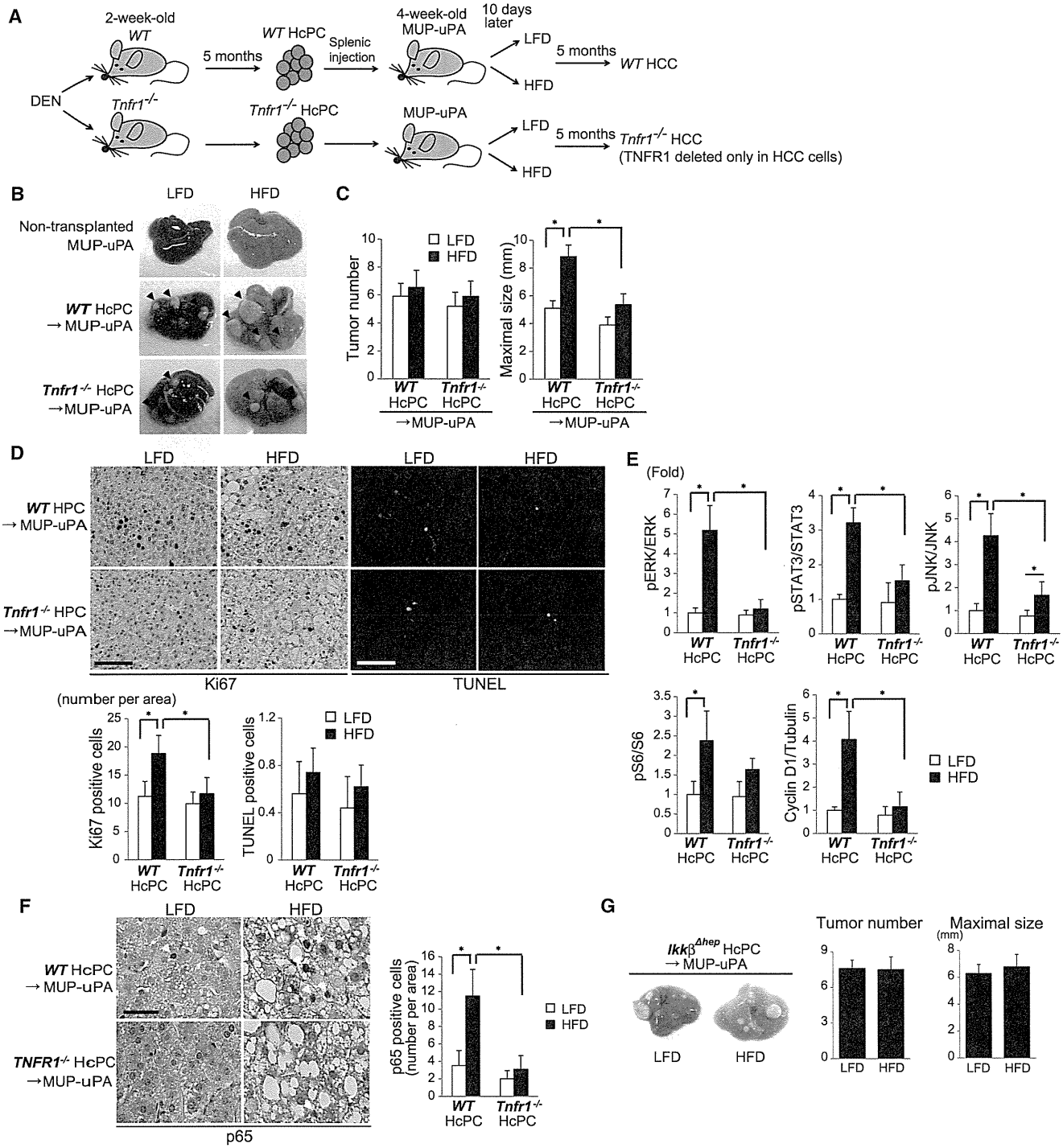


**Figure 6. TNFR1 Signaling Promotes Tumor Growth**

(A) HcPC isolation from DEN-treated *WT* and *Tnfr1*$^{-/-}$ mice and transplantation into *MUP-uPA* mice. HcPC-transplanted *MUP-uPA* mice were divided into two groups that were fed with either the LFD or HFD, and 5 months later tumorigenesis was assessed.

(B) Representative images of nontransplanted and HcPC-transplanted *MUP-uPA* mouse livers.

(C) Tumor numbers and maximal sizes. Results are means ± SEM (n = 10–11 per group). *p < 0.05.

(D) Ki67 IHC and TUNEL staining of tumor areas in livers in (C) (scale bar, 100 μm). Bars represent numbers of apoptotic and necrotic cells and Ki67-positive cells per field. Results are means ± SD (n = 6 per group). *p < 0.05.

(E) Tumor tissues from *WT* or *Tnfr1*$^{-/-}$ HcPC-transplanted *MUP-uPA* mice kept on the LFD or HFD were IB analyzed for phosphorylation of ERK, STAT3, JNK, and S6, and expression of cyclin D1. Data were quantified using Image J software and are presented as means ± SD (n = 5–6 per group). *p < 0.05.

*(legend continued on next page)*

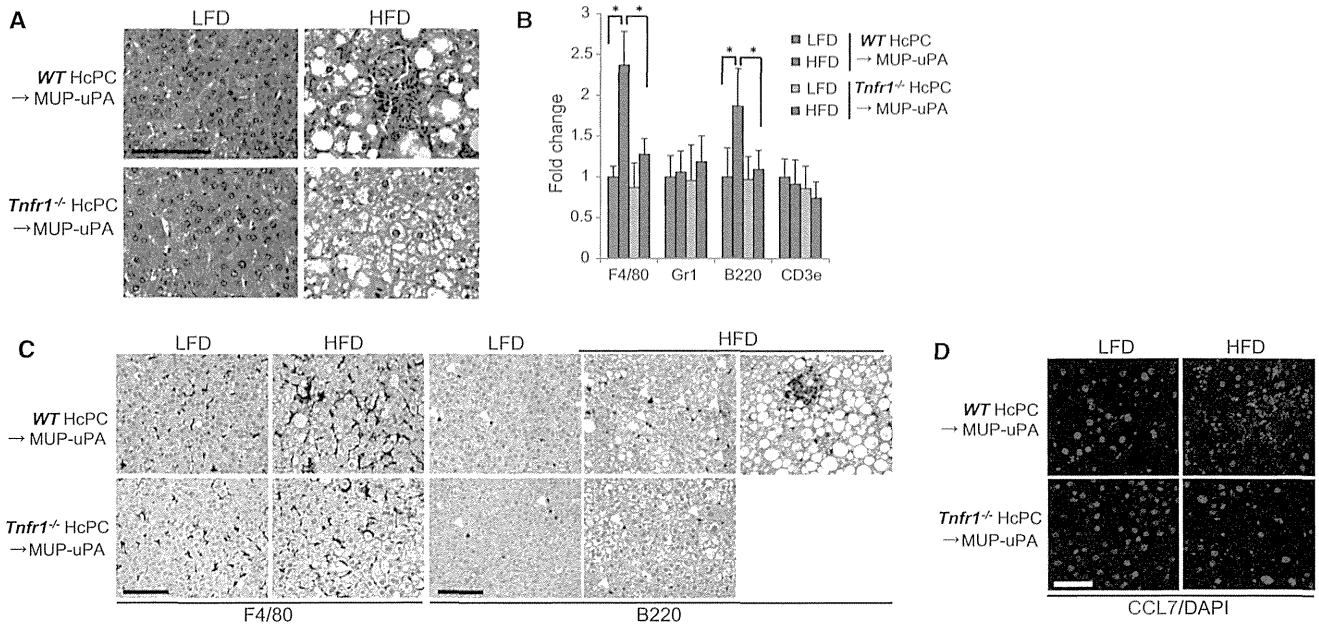


**Figure 7. TNFR1 Signaling in Cancer Cells Promotes Tumor-Elicited Inflammation**

(A) H&E analysis of tumors from *WT* or *Tnfr1*$^{-/-}$ HcPCs in *MUP-uPA* mice that were kept on the LFD or HFD (scale bar, 100 μm).

(B) Real-time PCR determination of immune cell marker mRNAs in tumor tissues. Data are means ± SD (n = 5 per group). *p < 0.05.

(C) IHC analysis of F4/80- and B220-positive cells in tumor tissues in (A) (scale bar, 100 μm).

(D) IF analysis of CCL7 expression in tumor tissues (scale bar, 25 μm).

See also Figure S7.

activation, but additional downstream TNFR1 effectors, such as JNK (Sakurai et al., 2008), may also contribute to HCC growth as well as hepatocyte death. TNF expression is also elevated in human NASH and anti-TNF therapy may reduce NASH activity (Schramm et al., 2008).

Although HFD feeding to *MUP-uPA* mice results in the upregulation of multiple cytokines and growth factors including several that stimulate HCC development, namely HGF and lymphotoxin (Haybaeck et al., 2009), anti-TNF therapy inhibited the obesity-enhanced progression of HcPCs to HCC and TNFR1 ablation almost completely blocked HCC development. We therefore suggest that anti-TNF drugs, perhaps in combination with improved intrahepatic delivery of chemical chaperons, such as TUDCA, should be evaluated for the inhibition of NASH-to-HCC progression and the treatment of steatohepatitic HCC along with more conventional chemotherapy.

## EXPERIMENTAL PROCEDURES

### Animals

*MUP-uPA* mice were kindly provided by E.P. Sandgren, University of Wisconsin-Madison (Weglarz et al., 2000). Liver-specific *Ikkβ*$^{\Delta hep}$ mice were described (Maeda et al., 2005). *Chop*$^{\Delta hep}$ mice were generated by crossing *Alb-Cre* mice with *Chop*$^{F/F}$ mice, which were developed by R.J.K together with Ira Tabas with the support of NIH grants DKD88227, DKD42394, and HLD52173. *Tnfr1*$^{-/-}$ mice were purchased from Jackson Laboratory (Bar Harbor). All animal studies were performed in accordance with NIH guidelines for the use and care of live animals and approved by University of California, San Diego (UCSD) Institutional Animal Care and Use Committee, S00218. All mouse lines were either on a pure C57BL/6 genetic background or crossed into it for at least ten generations. Studies were conducted on male mice maintained in filter-topped cages on autoclaved water and a regular chow diet (LFD, composed of 12% fat, 23% protein, and 65% carbohydrates based on caloric content) or a HFD (composed of 59% fat, 15% protein, and 26% carbohydrates based on caloric content; BioServ) according to UCSD and NIH guidelines.

### HcPC Isolation and Transplantation

DEN (Sigma) was i.p. injected into male mice (25 mg/kg) on postnatal day 14. After 5 months, HcPCs were isolated as described and transplanted into 4-week-old *MUP-uPA* (He et al., 2013).

### Primary Hepatocytes Cultures

Primary hepatocytes were isolated (He et al., 2013) and cultured in William's E medium with 10% fetal bovine serum (FBS) on collagen-coated plates. PA (Sigma) was dissolved in ethanol at 50°C and then diluted in BSA-containing RPMI-1640 medium that was applied to primary hepatocytes at a final concentration of 200 μM (to analyze signal transduction) or 300 μM (to analyze cell death).

(F) Activation of NF-κB analyzed by p65/RelA IHC in tumor tissues from *MUP-uPA* transplanted with *WT* or *Tnfr1*$^{-/-}$ HcPCs and kept on the LFD or HFD (scale bar, 25 μm). Bars show numbers of nuclear p65 positive cancer cells per 200× field. Data are means ± SD (n = 6 per group). *p < 0.05.

(G) Effect of IKKβ ablation on HFD-stimulated HcPC progression. HcPCs isolated from DEN-injected liver-specific *Ikkβ*$^{\Delta hep}$ were transplanted into *MUP-uPA* mice as in (A), and the HcPC-transplanted mice were kept on the LFD or HFD. After 5 months, tumor multiplicity and maximal sizes were determined. Data are means ± SEM (n = 10 per group).

See also Figure S6.

### Hepatic Lipid Profile

Hepatic lipids were extracted using chloroform/methanol (2:1 v/v), and TG and total cholesterol contents were measured using Triglyceride Reagent Set (Pointe Scientific) and Cholesterol E (Wako), respectively. FA composition was analyzed using gas chromatography at SRL, Tokyo.

### Biochemical Analyses and Reagents

Immunoblotting and real-time quantitative PCR (qPCR) were described (Maeda et al., 2005). Antibodies used were against phosphorylated ERK, ERK1/2, phosphorylated STAT3, STAT3, p-JNK, JNK1/2, phosphorylated S6, S6, p65, cyclinD1, and YAP (all from Cell Signaling); K19, GRP78, SREBP1, CHOP, CCL7, p62, and TNFR1 (all from Santa Cruz Biotechnology); p-eIF2α (Upstate); tubulin (Sigma); F4/80 (Molecular Probes); Ki67 (Gene Tex); AFP (Biocare Medical); TNF (R&D Systems); EpCAM (Abcam); and B220 (BD PharMingen). TUDCA and 4-PBA were from Calbiochem and Sigma, respectively. The GSH:GSSG ratio was analyzed using the GSSG/GSH Quantification Kit (Dojindo).

### Histology

Livers were fixed in 10% neutral-buffered formalin or 4% paraformaldehyde, embedded in paraffin, sectioned, stained with hematoxylin and eosin (H&E) and Sirius Red, and processed for IHC. For frozen-block preparation, tissue was embedded in Tissue-Tek OCT compound (Sakura Finetek). IHC and IF analyses were described (He et al., 2013). Stained areas were quantitated using Image J software. Slides were incubated with primary antibodies, followed by secondary antibodies labeled with Alexa488 or Alexa594 (Molecular Probes). TUNEL staining was performed using an Apoalert DNA Fragmentation Assay kit (Clontech). Accumulation of superoxide anions was examined by DHE staining (Sakurai et al., 2008). Tissue sample preparation and EM analysis were described (Lee et al., 2012).

### Infection of Recombinant Adenovirus

Primary hepatocytes were infected with recombinant adenovirus encoding β-galactosidase (LacZ) and GRP78 at a titer of 50 plaque-forming units/cell 4 hr after isolation.

### Statistical Analyses

Statistical analyses were performed using student's t test or one-way ANOVA followed by the Tukey-Kramer test for multiple comparisons. The number of tumors larger than 2 mm was counted for comparative analyses of tumor development. A p value $< 0.05$ indicated statistical significance.

## SUPPLEMENTAL INFORMATION

Supplemental Information includes seven figures and can be found with this article online at http://dx.doi.org/10.1016/j.ccr.2014.07.001.

## AUTHOR CONTRIBUTIONS

H.N. designed and performed the main experiments, and wrote the paper. A.U. designed and performed the main experiments. K.T., J.F.-B., D.D., H.O., and Z.Z. provided technical assistance for the main experiments. E.S. and K.K. discussed and interpreted the results from the study. R.J.K. discussed and interpreted the results from the study, and provided a mouse line and reagents for the completion of the studies. J.H. provided a mouse line. M.A.V. made the pathological diagnosis and provided images of human steatohepatitic HCC. M.K. conceived, supervised, and wrote the paper.

## ACKNOWLEDGMENTS

We thank Dr. E.P. Sandgren for *MUP-uPA,* Dr. I. Tabas for *Chop*$^{F/F}$ mice, and Dr. M.R. Mackey, Dr. G.A. Perkins, and Dr. M.H. Ellisman for help with the EM analysis. Research was supported by the Daiichi Sankyo Foundation of Life Science and Grant-in-Aid for Scientific Research (#25893042), and the Astellas Foundation for Research on Metabolic Disorders (H.N.); a Global Grant Scholarship from The Rotary Foundation (A.U.); a postdoctoral fellowship for Research Abroad, Research Fellowship for Young Scientists from the Japan Society for the Promotion of Science, and the Uehara Memorial Foundation Fellowship (K.T.); California Institute for Regenerative Medicine Stem Cell Training Grant II (TG2-01154; J.F.B.); the American Liver Foundation and a Young Investigator Award from the National Childhood Cancer Foundation "CureSearch" (D.D.); the Kanzawa Medical Research Foundation (H.O.); Cancer Research Institute Irvington Postdoctoral Fellowship (Z.Z.); grants from the NIH (CA155120-02 and CA118165-06; M.K.) and (DK042394-18, DK088227-06, and HL052173-16; R.J.K.), and Superfund Basic Research Program (P42ES010337; E.S. and M.K.). M.K. holds the Ben and Wanda Hildyard Chair for Mitochondrial and Metabolic Diseases and is an American Cancer Society Research Professor.

Received: January 2, 2014
Revised: May 28, 2014
Accepted: July 1, 2014
Published: August 14, 2014

## REFERENCES

Anderson, E.J., Lustig, M.E., Boyle, K.E., Woodlief, T.L., Kane, D.A., Lin, C.T., Price, J.W., III, Kang, L., Rabinovitch, P.S., Szeto, H.H., et al. (2009). Mitochondrial H2O2 emission and cellular redox state link excess fat intake to insulin resistance in both rodents and humans. J. Clin. Invest. *119*, 573–581.

Brunt, E.M. (2001). Nonalcoholic steatohepatitis: definition and pathology. Semin. Liver Dis. *21*, 3–16.

Caldwell, S., Ikura, Y., Dias, D., Isomoto, K., Yabu, A., Moskaluk, C., Pramoonjago, P., Simmons, W., Scruggs, H., Rosenbaum, N., et al. (2010). Hepatocellular ballooning in NASH. J. Hepatol. *53*, 719–723.

Calle, E.E., Teras, L.R., and Thun, M.J. (2005). Obesity and mortality. N. Engl. J. Med. *353*, 2197–2199.

Chen, C.L., Yang, H.I., Yang, W.S., Liu, C.J., Chen, P.J., You, S.L., Wang, L.Y., Sun, C.A., Lu, S.N., Chen, D.S., and Chen, C.J. (2008). Metabolic factors and risk of hepatocellular carcinoma by chronic hepatitis B/C infection: a follow-up study in Taiwan. Gastroenterology *135*, 111–121.

Cohen, J.C., Horton, J.D., and Hobbs, H.H. (2011). Human fatty liver disease: old questions and new insights. Science *332*, 1519–1523.

Day, C.P., and James, O.F. (1998). Steatohepatitis: a tale of two "hits"? Gastroenterology *114*, 842–845.

DeZwaan-McCabe, D., Riordan, J.D., Arensdorf, A.M., Icardi, M.S., Dupuy, A.J., and Rutkowski, D.T. (2013). The stress-regulated transcription factor CHOP promotes hepatic inflammatory gene expression, fibrosis, and oncogenesis. PLoS Genet. *9*, e1003937.

El-Serag, H.B. (2011). Hepatocellular carcinoma. N. Engl. J. Med. *365*, 1118–1127.

Farrell, G.C., van Rooyen, D., Gan, L., and Chitturi, S. (2012). NASH is an inflammatory disorder: pathogenic, prognostic and therapeutic implications. Gut Liver *6*, 149–171.

Goldstein, J.L., DeBose-Boyd, R.A., and Brown, M.S. (2006). Protein sensors for membrane sterols. Cell *124*, 35–46.

Haybaeck, J., Zeller, N., Wolf, M.J., Weber, A., Wagner, U., Kurrer, M.O., Bremer, J., Iezzi, G., Graf, R., Clavien, P.A., et al. (2009). A lymphotoxin-driven pathway to hepatocellular carcinoma. Cancer Cell *16*, 295–308.

He, G., Dhar, D., Nakagawa, H., Font-Burgada, J., Ogata, H., Jiang, Y., Shalapour, S., Seki, E., Yost, S.E., Jepsen, K., et al. (2013). Identification of liver cancer progenitors whose malignant progression depends on autocrine IL-6 signaling. Cell *155*, 384–396.

Holzer, R.G., Park, E.J., Li, N., Tran, H., Chen, M., Choi, C., Solinas, G., and Karin, M. (2011). Saturated fatty acids induce c-Src clustering within membrane subdomains, leading to JNK activation. Cell *147*, 173–184.

Hotamisligil, G.S. (2010). Endoplasmic reticulum stress and the inflammatory basis of metabolic disease. Cell *140*, 900–917.

Inami, Y., Waguri, S., Sakamoto, A., Kouno, T., Nakada, K., Hino, O., Watanabe, S., Ando, J., Iwadate, M., Yamamoto, M., et al. (2011). Persistent activation of Nrf2 through p62 in hepatocellular carcinoma cells. J. Cell Biol. *193*, 275–284.

Kammoun, H.L., Chabanon, H., Hainault, I., Luquet, S., Magnan, C., Koike, T., Ferré, P., and Foufelle, F. (2009). GRP78 expression inhibits insulin and ER stress-induced SREBP-1c activation and reduces hepatic steatosis in mice. J. Clin. Invest. *119*, 1201–1215.

Lee, A.H., Scapa, E.F., Cohen, D.E., and Glimcher, L.H. (2008). Regulation of hepatic lipogenesis by the transcription factor XBP1. Science *320*, 1492–1496.

Lee, J.H., Budanov, A.V., Talukdar, S., Park, E.J., Park, H.L., Park, H.W., Bandyopadhyay, G., Li, N., Aghajan, M., Jang, I., et al. (2012). Maintenance of metabolic homeostasis by Sestrin2 and Sestrin3. Cell Metab. *16*, 311–321.

Maeda, S., Kamata, H., Luo, J.L., Leffert, H., and Karin, M. (2005). IKKbeta couples hepatocyte death to cytokine-driven compensatory proliferation that promotes chemical hepatocarcinogenesis. Cell *121*, 977–990.

Malhi, H., and Kaufman, R.J. (2011). Endoplasmic reticulum stress in liver disease. J. Hepatol. *54*, 795–809.

Ota, T., Gayet, C., and Ginsberg, H.N. (2008). Inhibition of apolipoprotein B100 secretion by lipid-induced hepatic endoplasmic reticulum stress in rodents. J. Clin. Invest. *118*, 316–332.

Ozcan, U., Yilmaz, E., Ozcan, L., Furuhashi, M., Vaillancourt, E., Smith, R.O., Görgün, C.Z., and Hotamisligil, G.S. (2006). Chemical chaperones reduce ER stress and restore glucose homeostasis in a mouse model of type 2 diabetes. Science *313*, 1137–1140.

Park, E.J., Lee, J.H., Yu, G.Y., He, G., Ali, S.R., Holzer, R.G., Osterreicher, C.H., Takahashi, H., and Karin, M. (2010). Dietary and genetic obesity promote liver inflammation and tumorigenesis by enhancing IL-6 and TNF expression. Cell *140*, 197–208.

Puri, P., Mirshahi, F., Cheung, O., Natarajan, R., Maher, J.W., Kellum, J.M., and Sanyal, A.J. (2008). Activation and dysregulation of the unfolded protein response in nonalcoholic fatty liver disease. Gastroenterology *134*, 568–576.

Qiu, W., Zhang, J., Dekker, M.J., Wang, H., Huang, J., Brumell, J.H., and Adeli, K. (2011). Hepatic autophagy mediates endoplasmic reticulum stress-induced degradation of misfolded apolipoprotein B. Hepatology *53*, 1515–1525.

Rutkowski, D.T., Wu, J., Back, S.H., Callaghan, M.U., Ferris, S.P., Iqbal, J., Clark, R., Miao, H., Hassler, J.R., Fornek, J., et al. (2008). UPR pathways combine to prevent hepatic steatosis caused by ER stress-mediated suppression of transcriptional master regulators. Dev. Cell *15*, 829–840.

Sakurai, T., He, G., Matsuzawa, A., Yu, G.Y., Maeda, S., Hardiman, G., and Karin, M. (2008). Hepatocyte necrosis induced by oxidative stress and IL-1 alpha release mediate carcinogen-induced compensatory proliferation and liver tumorigenesis. Cancer Cell *14*, 156–165.

Salomao, M., Remotti, H., Vaughan, R., Siegel, A.B., Lefkowitch, J.H., and Moreira, R.K. (2012). The steatohepatitic variant of hepatocellular carcinoma and its association with underlying steatohepatitis. Hum. Pathol. *43*, 737–746.

Sandgren, E.P., Palmiter, R.D., Heckel, J.L., Daugherty, C.C., Brinster, R.L., and Degen, J.L. (1991). Complete hepatic regeneration after somatic deletion of an albumin-plasminogen activator transgene. Cell *66*, 245–256.

Schramm, C., Schneider, A., Marx, A., and Lohse, A.W. (2008). Adalimumab could suppress the activity of non alcoholic steatohepatitis (NASH). Z. Gastroenterol. *46*, 1369–1371.

So, J.S., Hur, K.Y., Tarrio, M., Ruda, V., Frank-Kamenetsky, M., Fitzgerald, K., Koteliansky, V., Lichtman, A.H., Iwawaki, T., Glimcher, L.H., and Lee, A.H. (2012). Silencing of lipid metabolism genes through IRE1α-mediated mRNA decay lowers plasma lipids in mice. Cell Metab. *16*, 487–499.

Soon, R.K., Jr., Yan, J.S., Grenert, J.P., and Maher, J.J. (2010). Stress signaling in the methionine-choline-deficient model of murine fatty liver disease. Gastroenterology *139*, 1730–1739.e1.

Tilg, H., and Moschen, A.R. (2010). Evolution of inflammation in nonalcoholic fatty liver disease: the multiple parallel hits hypothesis. Hepatology *52*, 1836–1846.

Toffanin, S., Friedman, S.L., and Llovet, J.M. (2010). Obesity, inflammatory signaling, and hepatocellular carcinoma–an enlarging link. Cancer Cell *17*, 115–117.

Wang, G., Yang, Z.Q., and Zhang, K. (2010). Endoplasmic reticulum stress response in cancer: molecular mechanism and therapeutic potential. Am J Transl Res *2*, 65–74.

Weglarz, T.C., Degen, J.L., and Sandgren, E.P. (2000). Hepatocyte transplantation into diseased mouse liver. Kinetics of parenchymal repopulation and identification of the proliferative capacity of tetraploid and octaploid hepatocytes. Am. J. Pathol. *157*, 1963–1974.

Xu, C., Bailly-Maitre, B., and Reed, J.C. (2005). Endoplasmic reticulum stress: cell life and death decisions. J. Clin. Invest. *115*, 2656–2664.

Virology 462-463 (2014) 42–48

Contents lists available at ScienceDirect

Virology

journal homepage: www.elsevier.com/locate/yviro

# The flavonoid apigenin inhibits hepatitis C virus replication by decreasing mature microRNA122 levels

Chikako Shibata [a], Motoko Ohno [a], Motoyuki Otsuka [a,b,*], Takahiro Kishikawa [a], Kaku Goto [c], Ryosuke Muroyama [c], Naoya Kato [c], Takeshi Yoshikawa [a], Akemi Takata [a], Kazuhiko Koike [a]

[a] Department of Gastroenterology, Graduate School of Medicine, The University of Tokyo, 5-3-1 Hongo, Bunkyo-ku, Tokyo 113-8655, Japan
[b] Japan Science and Technology Agency, PRESTO, Kawaguchi-shi, Saitama 332-0012, Japan
[c] Unit of Disease Control Genome Medicine, Institute of Medical Science, The University of Tokyo, Tokyo 108-8639, Japan

ARTICLE INFO

*Article history:*
Received 5 May 2014
Accepted 13 May 2014
Available online 14 June 2014

*Keywords:*
HCV
MicroRNA
Replicon
Polyphenol

ABSTRACT

Despite recent progress in the development of direct-acting antivirals against hepatitis C virus (HCV), chronic HCV infection remains an important health burden worldwide. MicroRNA122 (miR122), a liver-specific microRNA (miRNA), positively regulates HCV replication, and systemic application of antisense oligonucleotides against miR122 led to the long-lasting suppression of HCV viremia in human clinical trials. Here, we report that apigenin, a flavonoid and an inhibitor of maturation of a subset of miRNAs, inhibits HCV replication in vitro. Apigenin decreased the expression levels of mature miR122 without significantly affecting cell growth. Because supplementation of synthesized miR122 oligonucleotides or overexpression of constitutively active TRBP blocked these effects, the inhibitory effects of apigenin on HCV replication seemed to be dependent on the reduction of mature miR122 expression levels through inhibition of TRBP phosphorylation. Thus, apigenin intake, either through regular diet or supplements, may decrease HCV replication in chronically infected patients.



## Introduction

Hepatitis C virus (HCV) constitutes a significant health problem worldwide, with an estimated 130–170 million people chronically infected (Scheel and Rice, 2013). Chronic HCV infection leads to severe liver diseases, including advanced liver fibrosis, cirrhosis, and hepatocellular carcinoma (HCC). A recent HCV therapy consisting of a triple combination of pegylated interferon α (peg IFN-α), ribavirin, and protease inhibitors increased cure rates (Jacobson et al., 2011; Poordad et al., 2011; Bacon et al., 2011; Sherman et al., 2011). However, substantial side effects, resistance, and drug-drug interactions are concerns with this therapy. Although an IFN-free regimen with direct-acting antivirals (DAAs) is beginning to reach patients and increase cure rates (Manns and von Hahn, 2013; Deuffic-Burban et al., 2014), several issues remain, including treatment failure, resistant clones, and economic burden.

MicroRNA122 (miR122) is a highly abundant microRNA (miRNA) expressed in the liver and essential for the stability and propagation of HCV RNA (Jopling, 2012; Pfeffer and Baumert, 2010; Jopling et al., 2005). It binds to two closely spaced target sites in the highly conserved 5′-untranslated region (5′-UTR) of the HCV genome. These sites are conserved across all HCV genotypes and subtypes (Li et al., 2011). This positive regulation through 5′-UTR sites is a unique process, as compared to the usual function of miRNAs in the repression of gene expression via 3′-UTRs in target mRNAs. Although the precise mechanisms by which miR122 positively regulates HCV replication through its binding to the 5′-UTR of the HCV genome are not yet fully elucidated (Jopling, 2012), it was demonstrated that LNA-based anti-miR122 oligonucleotides led to the long-lasting suppression of HCV viremia and improvement of HCV-induced liver pathology in chimpanzees (Lanford et al., 2010). Based on experimental results, human clinical trials using miravirsen, an LNA-modified DNA phosphorothioate antisense oligonucleotide against miR122, have been conducted, and in Phase 2a studies miravirsen resulted in a dose-dependent reduction in HCV levels, without major adverse events and with no escape mutations in the miR122 binding sites of the HCV genome (Janssen et al., 2013). The miR122 binding sites are conserved across all HCV genotypes and subtypes, and miR122 could represent a host target for antiviral therapy.

We previously demonstrated that the flavonoid apigenin (4′,5,7-trihydroxyflavone) has inhibitory effects on the maturation of a subset of miRNAs and on subsequent miRNA function (Ohno et al., 2013). These effects were mediated by the inhibition of TRBP

* Corresponding author at: Department of Gastroenterology, Graduate School of Medicine, The University of Tokyo, 5-3-1 Hongo, Bunkyo-ku, Tokyo 113-8655, Japan. Tel.: +81 3 3815 5411x37966; fax: +81 3 3814 0021.
*E-mail address:* otsukamo-tky@umin.ac.jp (M. Otsuka).

http://dx.doi.org/10.1016/j.virol.2014.05.024

phosphorylation through inhibition of ERK activation (Ohno et al., 2013). We reported that the administration of apigenin to mice improved glucose intolerance induced by overexpression of miR103 in the liver, likely through suppression of mature miR103 expression. Moreover, we found that miR122 was also affected by apigenin (Ohno et al., 2013).

We hypothesized that apigenin may exert inhibitory effects on HCV replication by decreasing mature miR122 expression levels. In this study, we assessed the effects of apigenin on HCV replication and the possible molecular mechanisms by using an in vitro HCV replicon reporter system. Based on our findings, we propose potential novel management methods for chronic HCV infection and possibly other pathological states mediated by miR122.

## Results

### *Apigenin inhibits the biogenesis of miR122*

We recently showed that apigenin inhibits the biogenesis of a subset of miRNAs (Ohno et al., 2013). Because previous screening of the comprehensive miRNA expression changes revealed that miR122 was one of the miRNAs affected by apigenin (NCBI Gene Expression Omnibus (GEO) accession number: GSE46526) (Ohno et al., 2013), we here measured mature miR122 levels in Huh7 cells by quantitative RT-PCR, after apigenin treatment for 5 days. While the expression levels of let-7g, an unrelated miRNA, were not affected, apigenin significantly reduced mature miR122 expression levels in a dose-dependent manner (Fig. 1a). Northern blotting confirmed the reduced expression levels of miR122 after apigenin treatment (Fig. 1b). By contrast, expression of miR122 precursor, but not let-7g precursor, was increased after apigenin treatment (Fig. 1c), as we described previously (Ohno et al., 2013). Consistent with the reduced levels, miR122 function was inhibited by apigenin, as determined by the increased reporter values from a transiently transfected reporter construct with two miR122 target sites in tandem in its 3′-UTR (Fig. 1d). The effect was miR122 function-specific because no effects were observed with use of a reporter construct with mutations in the miR122 target sites (Fig. 1d). Apigenin had no significant effects on Huh7 cell growth at a final concentration of up to 5 μM (50 μM apigenin slightly reduced the cell number) (Fig. 1e). These results suggest that up to 5 μM of apigenin inhibits the expression levels of mature miR122 in Huh7 cells without affecting cell viability.

### *Apigenin inhibits HCV replication*

Because miR122 positively regulates HCV replication (Jopling et al., 2005), we hypothesized that apigenin might inhibit HCV replication by decreasing the expression levels of mature miR122. To test this hypothesis, we used Huh7 cells harboring an HCV replicon reporter construct (HCV-Feo), referred to as Huh7-Feo cells (Yokota et al., 2003). These cells continuously carry a replicon expressing a chimeric protein consisting of firefly luciferase and neomycin phosphotransferase under the HCV 5′ IRES and can be used to monitor intracellular HCV replication by measuring luciferase activity (Fig. 2a) (Yokota et al., 2003). Treatment of Huh7-Feo cells with apigenin (final concentration 5 or 50 μM) for 5 days significantly reduced HCV-Feo replication (Fig. 2b). The pattern of luciferase values closely matched the pattern of luciferase protein expression levels (Fig. 2c). The decrease in replication observed with 5 μM apigenin treatment was only slightly less than that obtained following the transfection of anti-miR122 oligonucleotides at 10 pM. Although 50 μM apigenin may have adverse effects on cell viability, as described above, these results suggest that 5 μM apigenin can significantly inhibit HCV replication without affecting cell viability, possibly through downregulation of mature miR122 expression levels.

### *Apigenin inhibits HCV replication through downregulation of miR122 levels*

To further investigate the mechanisms of the observed negative effects of apigenin on HCV replication, we applied synthesized mature miRNAs to Huh7-Feo cells to determine whether miRNA supplementation could antagonize the effects of apigenin. Overexpression of miR122 after the transfection of synthesized miR122, compared with the expression levels of miR122 in cells with no treatment or with let-7g transfection, was confirmed by Northern blotting (Fig. 2d). As expected, overexpression of miR122 efficiently antagonized the negative effects of apigenin on HCV replication, while supplementation of an unrelated miRNA, let-7g, had no effect on HCV replication (Fig. 2e). These results suggest that apigenin inhibits HCV replication by downregulating mature miR122 expression.

### *Phosphorylation mimic TRBP blocks the effects of apigenin*

Because we previously demonstrated that apigenin inhibits the maturation of a subset of miRNAs by inhibiting the phosphorylation of TRBP, which contributes to the maturation of a subset of miRNAs by binding to Dicer (Paroo et al., 2009). We constructed a flag-tagged TRBP-expressing construct and a phosphorylation mimics in which serine was substituted with aspartic acid (TRBP (SD)) (Paroo et al., 2009). The expression levels of the wild-type TRBP and TRBP(SD) constructs were comparable (Fig. 3a). After stably expressing these constructs in Huh7-Feo cells by lentiviral transduction, we determined the expression levels of miR122. While overexpression of wild-type TRBP slightly enhanced the expression levels of miR122, apigenin significantly reduced its expression levels (Fig. 3b). However, in TRBP(SD)-expressing cells, miR122 expression levels were significantly increased and were not affected by apigenin treatment (Fig. 3b), probably due to the phosphorylation mimic TRBP(SD) being constitutively active. Consistent with the changes in miR122 expression levels, replication of the HCV replicon, as determined by luciferase values, was inhibited by apigenin in cells expressing wild-type TRBP but not in cells expressing TRBP(SD), which showed a slight increase in replication (Fig. 3c). These results suggest that apigenin inhibits HCV replication through the inhibition of mature miR122 expression levels, probably by modulating TRBP phosphorylation, consistent with our previous report (Ohno et al., 2013).

## Discussion

In this study, we demonstrate that apigenin inhibits HCV replication by decreasing the expression levels of mature miR122, possibly through inhibition of the phosphorylation of TRBP, an important factor for the maturation of a subset of miRNAs (Paroo et al., 2009).

Our study revealed that apigenin inhibits HCV replication. A liver-specific miRNA, miR122, has been reported to be linked with pleiotropic physiological functions (Jopling, 2012; Otsuka et al., 2014), such as liver development, cholesterol metabolism, iron metabolism, and fatty acid metabolism (Takata et al., 2013a). A particularly intriguing function of miR122 is its role in promoting HCV replication (Jopling et al., 2005). The success of miravirsen, an LNA-modified DNA phosphorothioate antisense oligonucleotide against miR122, against HCV in a Phase 2a study (Janssen et al., 2013) shows its promise as a novel anti-HCV drug and as the first miRNA-targeting therapy to be trialed. While miravirsen hybridizes

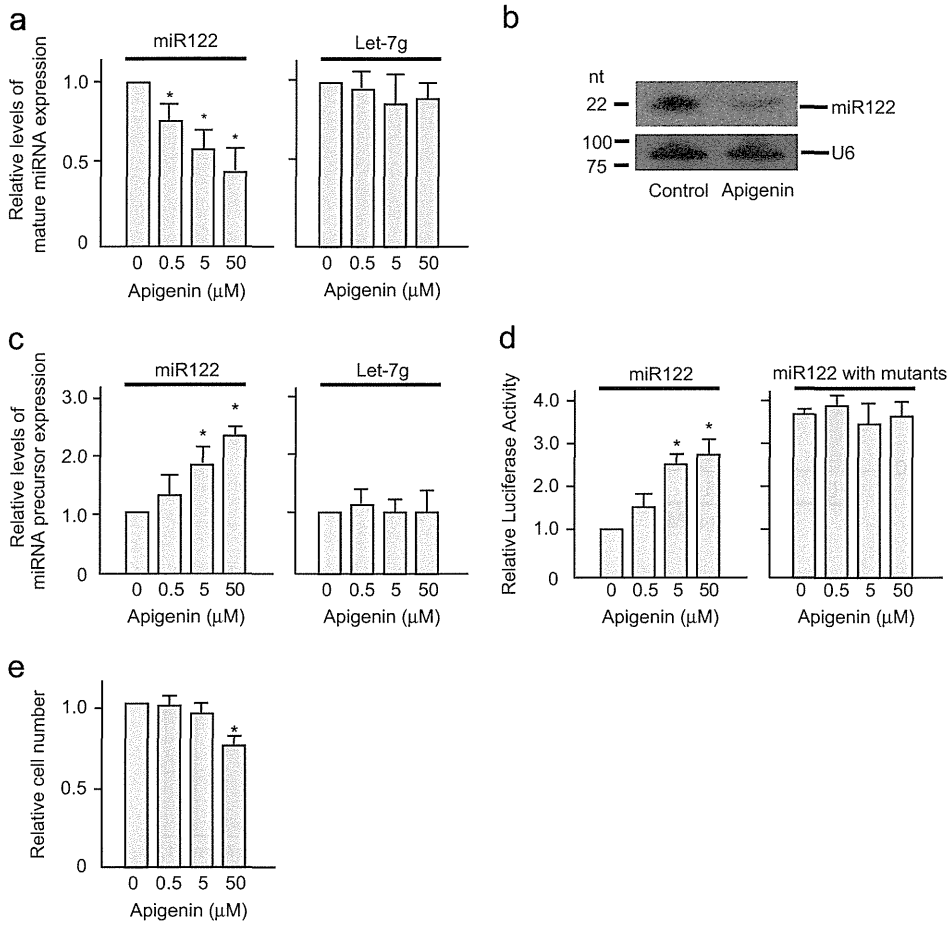


**Fig. 1.** Apigenin decreases mature miR122 expression levels. (a) The expression levels of mature miRNAs in Huh7 cells were determined by quantitative RT-PCR. Cells were treated with apigenin at the indicated doses for 5 days. Expression levels of mature miR122 and let-7g were determined. Relative expression levels are indicated as the means ± s.d. of three independent experiments. * $p < 0.05$. (b) The expression levels of mature miR122 were determined by Northern blotting. Huh7 cells were treated with 5 μM apigenin for 5 days. Expression levels of mature miR122 were determined by Northern blotting. U6 levels were determined as a loading control by reprobing the same membrane. Representative results from three independent experiments are shown. (c) The expression levels of miRNA precursors in Huh7 cells were determined by quantitative RT-PCR. Cells were treated with apigenin at the indicated doses for 5 days. Expression levels of miR122 and let-7g precursors were determined. Relative expression levels are indicated as the means ± s.d. of three independent experiments. * $p < 0.05$. (d) Endogenous miR122 function was determined by reporter assay. Huh7 cells were transiently transfected with reporter constructs containing miR122 binding sites or mutants. Cells were treated with apigenin at the indicated doses for 36 h. Data represent the mean ± s.d. of three independent experiments. * $p < 0.05$. (e) The number of cells was counted after treatment with apigenin at the indicated doses for 5 days. Experiments were performed in duplicate in a single test and the data represent the means ± s.d. of three independent tests. * $p < 0.05$.

to the 5′ region of mature miR122, resulting in sequestration and inhibition of miR122 (Janssen et al., 2013), it also binds to the stem-loop structure of pri- and pre-miR-122 and inhibits both Dicer- and Drosha-mediated processing of miR122 precursors (Gebert et al., 2014). Therefore, the importance of miR122 in HCV replication appears to depend on its expression level as well as its binding capacity. Because apigenin reduced the expression levels of mature miR122, and supplementation of synthesized mature miR122 blocked the effects of apigenin on HCV replication, the inhibitory effects of apigenin on HCV replication seem to be dependent on reduced levels of mature miR122. However, other potential molecular mechanisms for the effects of apigenin on HCV replication may exist.

Apigenin decreased the expression levels of a subset of mature miRNAs, including miR122, similar to the case of miR103, as we observed previously using microarray analyses (GEO accession number: GSE46526) (Ohno et al., 2013). We reported that the decreased maturation of miR103 was due to decreased phosphorylation of TRBP resulting from inhibition of ERK activities (Paroo et al., 2009). Because overexpression of the TRBP(SD) increased the levels of mature miR122, it appears that the reduced maturation of miR122 was also dependent on the activity of TRBP, which was inhibited by apigenin (Ohno et al., 2013). However, mature miRNA levels might be regulated not only by their synthesis but also, potentially, by their degradation, although this has not yet been established definitively (Jopling, 2012), and the effects of apigenin on the levels of mature miRNAs may be more diverse than expected. These effects should be explored in future studies involving the identification of the specific molecular target with which apigenin directly interacts and the development of an apigenin synthesis method, as has been achieved for resveratrol, another pleiotropic polyphenol (Snyder et al., 2011).

miR122 levels are frequently reduced in HCC compared with background liver tissues (Hou et al., 2011; Kutay et al., 2006; Gramantieri et al., 2007; Tsai et al., 2009), and lower miR122 expression levels in HCC tissues are correlated with a poor prognosis (Kojima et al., 2011). Because mice lacking miR122 in the liver showed spontaneous inflammation and liver tumors (Hsu et al., 2012; Tsai et al., 2012), miR122 may function as a tumor suppressor. However, to date no detectable liver toxicity has been reported with antisense oligonucleotide inhibition of miR122 in mice, primates, or humans (Lanford et al., 2010; Janssen et al., 2013; Elmén et al., 2008; Krützfeldt et al., 2005). We reported previously that transgenic mice expressing an antisense oligonucleotide specific for

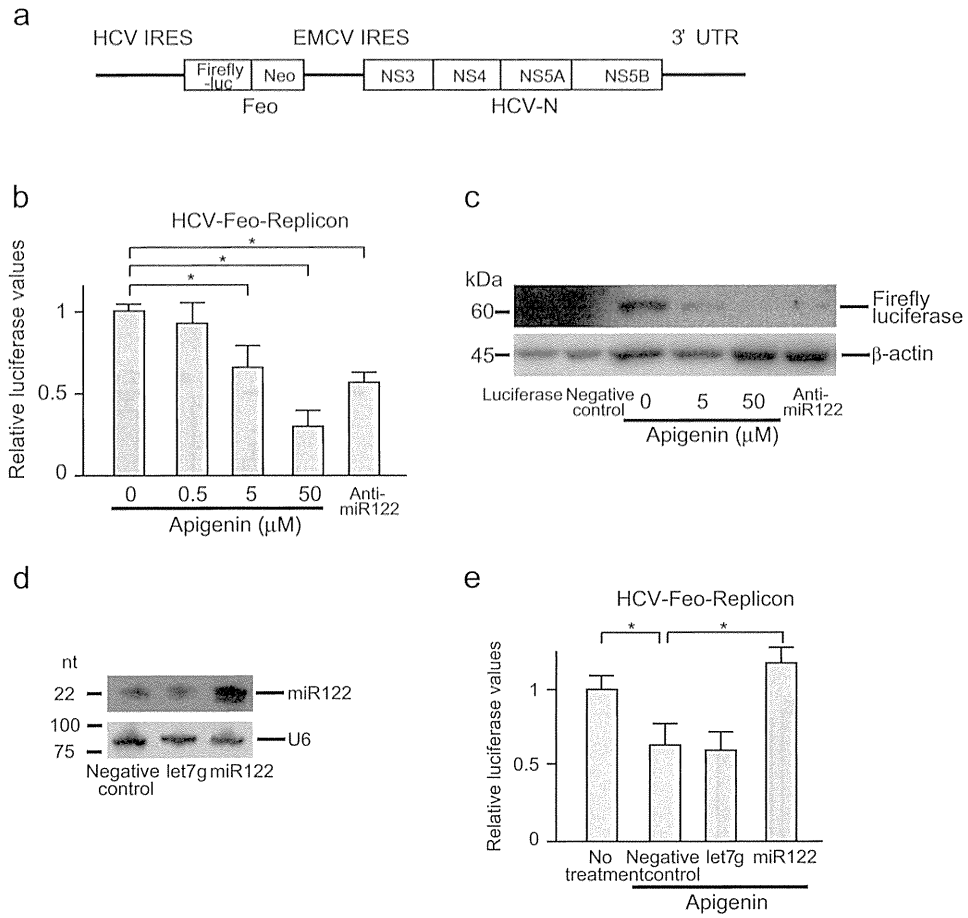


**Fig. 2.** Apigenin inhibits HCV replication in vitro by modulating miR122 levels. (a) Structure of the HCV replicon reporter. IRES, internal ribosomal entry site; firefly-luc, firefly luciferase gene; neo, neomycin resistance gene. NS3, NS4, NS5A, NS5B, and HCV are nonstructural proteins. Fusion genes consisting of the firefly luciferase gene and neomycin resistance gene are referred to as Feo. Huh7-Feo cells harbor an HCV replicon reporter construct (HCV-Feo) and expresses a chimeric protein consisting of firefly luciferase and neomycin phosphotransferase under the HCV 5′ IRES. (b) Apigenin inhibited replication of the HCV replicon reporter construct. Huh7-Feo cells were treated with apigenin for 5 days and the luciferase values were determined. Synthesized anti-miR122 oligonucleotides were transfected as a reference. Data represent the means ± s. d. of three independent experiments. * $p < 0.05$. (c) Apigenin inhibits the expression of luciferase protein under the HCV 5′ IRES of the reporter construct. Huh7-Feo cells were treated as described in (b) and luciferase protein was quantified by Western blotting. 293T cell lysates obtained after transient transfection with luciferase-expressing plasmid or control plasmid were used as controls. Representative results from three independent experiments are shown. (d) and (e) Synthesized miR122 blocks the inhibitory effects of apigenin on HCV replication. Synthesized mature miR122 and let-7g were transfected into Huh7-Feo cells. (d) Cells were harvested 48 h after transfection and mature miR122 levels were determined by Northern blotting. U6 levels were used as a loading control. Representative results from three independent experiments are shown. Synthesized miR122 overexpression blocked the inhibitory effects of apigenin on HCV replication (e) Huh7-Feo cells were treated or not treated with 5 μM apigenin for 5 days. Synthesized miRNAs were transfected 48 h before measurement. Luciferase values for HCV-Feo were determined by reporter assay. Data represent the means ± s.d. of the absolute luciferase values of three independent experiments. * $p < 0.05$.

miR122 showed no spontaneous pathological features (Kojima et al., 2011). In addition, mice treated with apigenin for 2 weeks suffered no detectable harmful events in our previous studies (Ohno et al., 2013). Therefore, while several miRNAs other than miR103 and miR122 are affected by apigenin (Ohno et al., 2013), apigenin treatment in vivo seems to be a safe and convenient method of reducing the expression levels of a subset of miRNAs. One of the reasons for this is that the effects of apigenin are relatively mild; it reduces but does not completely abolish target miRNA expression levels. The effects of apigenin as well as its long-term safety need to be determined in a small animal model.

The appropriate dose of apigenin in this in vitro study was 5 μM. The fasting plasma concentration of flavonoids, including apigenin, is proportional to their intake. Intake of 100 mg flavonoids results in a plasma concentration of ~410 nM (Cao et al., 2010). Apigenin is abundant in parsley, celery, and other herbs, according to the USDA Database for the Flavonoid Content of Selected Foods (Release 3.1). For example, fresh parsley contains 215.46 mg apigenin per 100 g edible portion, dried parsley contains 4303.50 mg, and celery seeds contain 78.65 mg. The plasma concentration of apigenin theoretically reaches 1.7 μM, assuming one eats 10 g of dried parsley per day. Thus, although it is not impossible to reach a plasma apigenin concentration of 5 μM through normal dietary intake, apigenin supplementation may be required to obtain an appropriate dose. However, the apigenin concentration in the liver may be higher than the plasma due to direct blood flow from the intestine, which absorbs nutrients, and eating foods rich in apigenin may be sufficient to reach the appropriate liver concentration. The concentration of apigenin in liver tissues should thus be determined in future studies.

In HCV therapy, treatment has become more effective with the advent of DAAs (Scheel and Rice, 2013; Manns and von Hahn, 2013). Thus, it is uncertain the extent to which our finding, that apigenin may inhibit HCV replication, contributes to patient care in the DAA era. However, worldwide access to drugs and the implementation of economical therapy are major challenges (Scheel and Rice, 2013; Manns and von Hahn, 2013), in addition to cases of non-responders and patients with clones resistant to DAAs. Our findings may provide novel insights into HCV management. The combination of apigenin with other agents, including